https://ntrs.nasa.gov/search.jsp?R=19920007094 2020-03-17T12:56:21+00:00Z

P-55

ROBUST CONTROL OF SYSTEMS WITH REAL PARAMETER UNCERTAINTY AND UNMODELLED DYNAMICS

NASA Research Grant NAG-1-1102

Annual Progress Report

Prepared by:

Principal Investigator:
Bor-Chin Chang
Department of Mechanical Engineering and Mechanics
Drexel University
Philadelphia, PA 19104
(215) 895-1790

and

Co-Principal Investigator:
Robert Fischl
Department of Electrical Engineering
Drexel University
Philadelphia, PA 19104
(215) 895-2254

October 1991

(NASA-CR-189284) ROBUST CONTROL OF SYSTEMS WITH REAL PARAMETER UNCERTAINTY AND UNMODELLED DYNAMICS Annual Progress Report (Drexel Univ.) 55 p

N92-16312

CSCL 13I

Unclas

G3/37 0084078

ABSTRACT

During this research period we have made significant progress in the four proposed areas: (1) Design of robust controllers via H^∞ optimization, (2) Design of robust controllers via mixed H^2/H^∞ optimization, (3) M-Δ Structure and robust stability analysis for structured uncertainties, and (4) A study on controllability and observability of perturbed plant.

It is well known now that the two-Riccati-equation solution to the H^∞ control problem can be used to characterize all possible stabilizing optimal or suboptimal H^∞ controllers if the optimal H^∞ norm or γ, an upper bound of a suboptimal H^∞ norm, is given. In this research, we discovered some useful properties of these H^∞ Riccati solutions. Among them, the most prominent one is that the spectral radius of the product of these two Riccati solutions is a continuous, nonincreasing, convex function of γ in the domain of interest. Based on these properties, quadratically convergent algorithms are developed to compute the optimal H^∞ norm. We also set up a detailed procedure for applying the H^∞ theory to robust control systems design. The relationship between the H^∞ norm and robustness issues has been carefully reviewed and the guidelines to formulate H^∞ optimization problems including the construction of a state-space realization of the generalized plant have been established. The controller formulas of Glover and Doyle are slightly modified and used to construct an optimal controller without any numerical difficulty.

The desire to design controllers with H^∞ robustness but H^2 performance has recently resulted in mixed H^2 and H^∞ control problem formulation. The mixed H^2/H^∞ problem have drawn attentions of many investigators. However, solution is only available for special cases of this problem. We formulated a relatively realistic control problem with H^2 performance index and H^∞ robustness constraint into a more general mixed H^2/H^∞ problem. No optimal solution yet is available for this more general mixed H^2/H^∞ problem. Although the optimal solution for this mixed H^2/H^∞ control has not yet been found, we proposed a design approach which can be used through proper choice of the available design parameters to influence both robustness and performance.

For a large class of linear time-invariant systems with real parametric perturbations, the coefficient vector of the characteristic polynomial is a multilinear function of the real parameter vector. Based on this multilinear mapping relationship together with the recent

developments for polytopic polynomials and parameter domain partition technique, we proposed an iterative algorithm for computing the real structured singular value. The algorithm requires neither frequency search nor Routh's array symbolic manipulations and allows the dependency among the elements of the parameter vector. Moreover, the number of the independent parameters in the parameter vector is not limited to three as is required by many existing structured singular value computation algorithms.

For task 4, the work during this period concentrated on developing software for investigating the controllability robustness of linear time invariant systems. A preliminary software package (described in Appendix A) was developed for measuring the size, shape and location of the recovery region of initial states in finite time by bounded control. Although the various optimization algorithms (needed to automatically obtain the value of the indicators) work, they need to be refined in order to take care of such problems as ill-conditioned recovery regions.

TABLE OF CONTENTS

PROGRESS REPORT

ROBUST CONTROL OF SYSTEMS WITH REAL PARAMETER UNCERTAINTY AND UNMODELLED DYNAMICS

1. INTRODUCTION

This document is the second-period progress report on the NASA supported research, "Robust Control of Systems with Real Parameter Uncertainty and Unmodelled Dynamics", (No. NAG-1-1102). We are happy to report that in this research period we have made significant progress in the following proposed research problems: (1) Design of robust controllers via H^∞ optimization, (2) Design of robust controllers via mixed H^2/H^∞ optimization, (3) M-Δ Structure and robust stability analysis for structured uncertainties, and (4) A study on controllability and observability of perturbed plant.

Doyle, Glover, Khargonekar, and Francis (abbr.: DGKF) [1], and Glover and Doyle [2] presented a celebrating two-Riccati-equation type solution to a standard H^∞ control problem. The two-Riccati-equation method characterizes all possible stabilizing suboptimal H^∞ controllers whose order is not higher than that of the plant. The suboptimal H^∞ controller formulas in [1], [2] can be easily transformed into descriptor forms to construct optimal H^∞ controllers without numerical difficulties if the optimal H^∞ norm is given. The optimal H^∞ controllers, with very few exceptions, have direct feedthrough terms and therefore infinite bandwidth. Hence, control engineers may prefer strictly proper suboptimal H^∞ controllers to the optimal ones. However, knowing the optimal H^∞ norm is important in determining which suboptimal controller to be chosen in practical design.

Recently, an efficient algorithm for computing the optimal H^∞ norm was proposed by Scherer [3]. Scherer considered the inverse (or pseudo inverse) of the DGKF H^∞ Riccati solutions, $X_\infty(\gamma)$ and $Y_\infty(\gamma)$, defined a new independent variable $\mu = \gamma^{-2}$, and showed that these inverses are concave functions of μ in matrix sense on their domains of definition. Based on this fact, a quadratically convergent Newton-like algorithm was proposed to compute the optimal H^∞ norm.

Pandey et. al.'s hybrid gradient-bisection method [4] and Chang et. al.'s double secant and bisection method [5] were also proposed for the computation of the optimal H^∞ norm. The significance of the conjecture that $\rho[X_\infty(\gamma)Y_\infty(\gamma)]$, the spectral radius of $X_\infty(\gamma)Y_\infty(\gamma)$, is a convex function of γ^2 was mentioned in these two papers. Since there was no proof for this conjecture, bisection was used in these two algorithms as supplement

to guarantee convergence.

In this research period, we discovered several important properties of the two DGKF H^∞ Riccati solutions, $X_\infty(\gamma)$ and $Y_\infty(\gamma)$. Among them, the most prominent one is that $\rho[X_\infty(\gamma)Y_\infty(\gamma)]$ is a continuous, nonincreasing, convex function of γ on (β, ∞), where β is the infimum of γ such that the two DGKF H^∞ Riccati solutions, $X_\infty(\gamma)$ and $Y_\infty(\gamma)$, exist and are positive semidefinite. Based on this property, a quadratically convergent algorithm can be easily developed to compute the optimal H^∞ norm, i.e., the γ_∞ such that $\rho[X_\infty(\gamma_\infty)Y_\infty(\gamma_\infty)] = \gamma_\infty^2$ if a starting γ is given inside the interval (β, γ_∞), i.e., $\gamma > \beta$ and $\rho[X_\infty(\gamma)Y_\infty(\gamma)] > \gamma^2$.

A γ inside the interval (β, γ_∞) most of the time can be easily found without the knowledge of β. However, the computation of β can be necessary if β itself is the optimum, which occurs when $\rho[X_\infty(\beta)Y_\infty(\beta)] < \beta^2$. Newton-Raphson's method can be employed to compute β and the convergence is quadratic.

H^∞ control theory can handle the following two robustness issues: (1) Minimization of the maximum error energy for all command/disturbance inputs with bounded energy, and (2) Closed-loop stability under unstructured plant uncertainties with bounded H^∞ norm. Besides, H^∞ control theory is also indispensable in the structured singular value treatment of structured plant uncertainties [6,7]. Detailed procedures to formulate these robust control problems into H^∞ optimization problems will be given in the report.

For most practical control systems, a particular performance index is usually of considerable interest. At the same time there is also a desire to improve on the closed-loop system robustness. However, it is well known that there exists a tradeoff between these two design objective. Any improvement gained in one of the design goals is usually accompanied by a loss in the other. The Linear Quadratic Gaussian (LQG) Theory has been used successfully to design observer-based controllers with optimal performance for plants with fixed (or fixed power spectrum) exogenous signals. It is well known however, that the controllers derived using this approach possess poor robustness properties when compared to the guaranteed stability margins provided by full-state feedback control. Doyle and Stein [8, 9] devised a procedure, usually referred to in the literature as the Loop Transfer Recovery (LTR), to asymptotically recover the full-state feedback loop by tuning the LQG designed observer. The adjustment procedure is achieved by introducing a fictitious noise to the nominal plant input. A new LQG observer based controller is then derived. For the case of minimum-phase plants, the asymptotic recovery is achieved by letting the intensity of the added fictitious noise approach infinity. The procedure however,

has limitations when applied to nonminimum phase plants.

In this research we concentrate on the recently developed H^∞ theory which evolved from the sensitivity minimization problem formulated by Zames [10]. It was shown there that many of the classical design objectives can be incorporated in the H^∞ design. For instance, the modeling of plant uncertainties can easily be formulated in terms of normed H^∞ plant neighborhoods. Another advantage of this relatively new theory can be revealed in the flexibility it offers to the designer in the formulation of the problem. For example, the well known design methodology of loop shaping can easily be achieved via the choice of frequency dependent weights on input as well as output signals. Although no direct relations between these two are known, with the new state-space solution to the general H^∞ problem [1, 2, 11] the design approach as will be shown later reduces to simply varying certain design parameters in order to achieve the design objectives.

The motivation to design controllers for desired H^2 performance with H^∞ robustness constraints has recently resulted in mixed H^2 and H^∞ control problem formulation [11, 12, 13, 14]. Special cases of this problem have been studied there and a solution in the form of coupled Riccati equations has been proposed. Although the optimal solution for this mixed H^2/H^∞ control has not yet been found, we proposed a design approach which can be used through proper choice of the available design parameters to influence both robustness and performance.

Stability robustness is an important issue in the analysis and design of control systems. Currently, there are two major approaches to stability robustness analysis. One is the structured-singular-value (SSV) [6,7] or the multivariable-stability-margin (MSM) [15,16] approach and the other is the perturbed-characteristic-polynomials approach [17-22]. Several significant progresses have been made in both approaches. In this research, an iterative algorithm of computing the real SSV and the real MSM is developed based on the existing results in both approaches.

For a large class of linear time-invariant systems with real parametric perturbations, the coefficient vector of the characteristic polynomial is a multilinear function of the real parameter vector. Based on this multilinear mapping together with the recent results by De Gaston and Safonov [15], Sideris and Pena [16], Bartlett, Hollot, and Lin [18], and Bouguerra, Chang, Yeh, and Banda [23], an algorithm for computing the real structured singular value is proposed. The algorithm requires neither frequency search nor Routh's array symbolic manipulations and allows the dependency among the elements of the parameter vector. Moreover, the number of the independent parameters in the parameter

vector is not limited to three, as is required by many existing structured singular value computation algorithms.

The literature on controllability gives various degree of controllability (DOC) measures, each based on different point of view. That is either, in terms of the controllability grammian or the recovery region of initial states in finite time by bounded control, or the variation of the system and control matrices. The work during this period concentrated on: (i) trying to develop a relation between the various DOC measures encountered in the literature, and (ii) developing software for investigating the controllability robustness of linear time invariant systems. A preliminary software package (described in Appendix A) was developed for measuring the size, shape and location of the recovery region. Although the various optimization algorithms (needed to automatically obtain the value of the indicators) work, they need to be refined in order to take care of such problems as ill-conditioned recovery regions.

In section 2 of this report, we will show the overall progress in this research period. The work performed and the status of the proposed tasks are summarized in section 3. Section 4 is the conclusion. The work for future research will also be briefly described in section 4.

2. OVERALL PROGRESS

Consider the system

$$\begin{bmatrix} z(s) \\ y(s) \end{bmatrix} = \begin{bmatrix} G_{11}(s) & G_{12}(s) \\ G_{21}(s) & G_{22}(s) \end{bmatrix} \begin{bmatrix} v(s) \\ u(s) \end{bmatrix} := G(s) \begin{bmatrix} v(s) \\ u(s) \end{bmatrix} \tag{2-1a}$$

$$u(s) = K(s)\, y(s) \tag{2-1b}$$

where $G_{11}(s) \in \mathbb{R}(s)^{p_1 x m_1}$, $G_{12}(s) \in \mathbb{R}(s)^{p_1 x m_2}$, $G_{21}(s) \in \mathbb{R}(s)^{p_2 x m_1}$, and $G_{22}(s) \in \mathbb{R}(s)^{p_2 x m_2}$. $\mathbb{R}(s)^{pxm}$ is the set of pxq proper rational matrices with real coefficients. Recall that the standard H^∞ optimization problem is the problem of finding a proper controller K(s) such that the closed-loop system is internally stable and $\|T_{zv}\|_\infty$ is minimized where $T_{zv}(s)$ is the transfer function of the closed-loop system from v to z.

The realization of the generalized plant G(s) is given by

$$G(s) = \left[\begin{array}{c|cc} A & B_1 & B_2 \\ \hline C_1 & D_{11} & D_{12} \\ C_2 & D_{21} & D_{22} \end{array}\right] \tag{2-2}$$

with the following assumptions:

(i) $(\hat{C}_1, \hat{A})$ has no unobservable modes on jω-axis and $(\tilde{A}, \tilde{B}_1)$ has no uncontrollable modes on jω-axis, where

$$\hat{A} = A - B_2 D_{12}^T C_1, \tag{2-3a}$$

$$\hat{C}_1 = C_1 - D_{12} D_{12}^T C_1, \tag{2-3b}$$

$$\tilde{A} = A - B_1 D_{21}^T C_2, \tag{2-3c}$$

$$\tilde{B}_1 = B_1 - B_1 D_{21}^T D_{21}. \tag{2-3d}$$

(ii) $D_{11} = 0, \quad D_{12} = \begin{bmatrix} 0 \\ I \end{bmatrix}, \quad D_{21} = [\, 0 \quad I \,], \quad D_{22} = 0.$

(iii) (A, B_2) is stabilizable and (C_2, A) is detectable.

The two Riccati equations involved in the H^∞ solution can be expressed as:

$$\hat{A}^T X_\infty + X_\infty \hat{A} + X_\infty (\gamma^{-2} B_1 B_1^T - B_2 B_2^T) X_\infty + \hat{C}_1^T \hat{C}_1 = 0 \tag{2-4a}$$

and

$$\tilde{A} Y_\infty + Y_\infty \tilde{A}^T + Y_\infty (\gamma^{-2} C_1^T C_1 - C_2^T C_2) Y_\infty + \tilde{B}_1 \tilde{B}_1^T = 0, \tag{2-4b}$$

where $\hat{A}$, $\tilde{A}$, $\tilde{B}_1$ and $\hat{C}_1$ are defined on (2-3).

The following theorem characterizes suboptimal stabilizing controllers such that $\|T_{zv}\|_\infty < \gamma$.

DGKF Theorem : [1]

There exists a stabilizing controller such that $\|T_{zv}\|_\infty < \gamma$ if and only if the following three conditions hold.

(i) There exists a positive semidefinite stabilizing solution $X_\infty(\gamma)$ to (2-4a). (2-5a)

(ii) There exists a positive semidefinite stabilizing solution $Y_\infty(\gamma)$ to (2-4b). (2-5b)

(iii) $\rho[X_\infty(\gamma) Y_\infty(\gamma)] < \gamma^2$. (2-5c)

Moreover, when these conditions hold, one such controller is

$$K_{sub}(s) = \left[\begin{array}{c|c} A_k & B_k \\ \hline C_k & 0 \end{array}\right] \tag{2-6}$$

with

$$B_k = -EL_2, \qquad C_k = F_2,$$

$$A_k = A + \begin{bmatrix} B_1 & B_2 \end{bmatrix}\begin{bmatrix} F_1 \\ F_2 \end{bmatrix} + EL_2(C_2+D_{21}F_1),$$

where

$$E = (I- \gamma^{-2}Y_\infty X_\infty)^{-1}, \quad F_1 = -B_1^T X_\infty, \quad F_2 = -B_2^T X_\infty - D_{12}^T C_1,$$

$$L_1 = \gamma^{-2}Y_\infty C_1^T, \qquad L_2 = -Y_\infty C_2^T - B_1 D_{21}^T.$$

The above theorem shows an easy state-space approach to construct a stabilizing suboptimal controller such that $\|T_{zv}\|_\infty < \gamma$. The theorem can also be used to compute the optimal H^∞ norm and construct an optimal H^∞ controller. The optimal $\|T_{zv}\|_\infty$ is the infimum of γ such that the above three conditions hold. With very few exceptions, the optimum occurs when $\rho[X_\infty(\gamma)Y_\infty(\gamma)] = \gamma^2$ which will render A_k and E undefined. This numerical difficulty can be easily resolved by transforming (2-6) into a descriptor form [1][25][26].

2.1 PROPERTIES OF H^∞ RICCATI SOLUTIONS

First, we assume $(C_1, -A)$ is detectable. This assumption will be removed later in this section. Suppose we have Riccati equation

$$\hat{X}A^T + A\hat{X} + (\gamma^{-2}B_1B_1^T - B_2B_2^T) + \hat{X}C_1^TC_1\hat{X} = 0, \tag{2-7}$$

then solution $\hat{X}(\gamma)$ has following properties.

Theorem 2.1: $\hat{X}(\gamma)$ is a well-defined function on $(\alpha_x, +\infty)$, where

$$\alpha_x := \inf\{\gamma : \gamma \in \mathbb{R}_+ \text{ and } \hat{X}(\gamma) \text{ exists}\} \tag{2-8}$$

Moreover, $\hat{X}(\gamma)$ is analytic with

$$\dot{\hat{X}}(\gamma) := \frac{d}{d\gamma}(\hat{X}(\gamma)) \geq 0 \tag{2-9}$$

$$\ddot{\hat{X}}(\gamma) := \frac{d^2}{d\gamma^2}(\hat{X}(\gamma)) \le 0 \tag{2-10}$$

on $(\alpha_x, +\infty)$.

Furthermore, the following theorem gives the eigen properties of $\hat{X}(\gamma)$.

Theorem 2.2: On $(\alpha_x, +\infty)$,

a) all eigenvalues of $\hat{X}(\gamma)$ are smooth, nondecreasing functions of γ;

b) the minimal eigenvalue of $\hat{X}(\gamma)$ is a nondecreasing, concave function of γ;

c) $\hat{X}(\gamma)$ is invertible almost everywhere.

This theorem implies that if we define

$$\beta_x := \inf \{\gamma: \gamma \in \mathbb{R}_+ \text{ and } \hat{X}(\gamma) \text{ is positive semidefinite}\}, \tag{2-11}$$

then either $\lambda_{min}[\hat{X}(\beta_x)] = 0$ or $\beta_x = \alpha_x$, which in turn implies $\hat{X}(\gamma)$ is positive definite everywhere on $(\beta_x, +\infty)$.

With these properties of $\hat{X}(\gamma)$ in mind, one can easily find the corresponding properties of $X_\infty(\gamma)$ by comparing the following two equations.

$$A^T X_\infty + X_\infty A + X_\infty(\gamma^{-2} B_1 B_1^T - B_2 B_2^T) X_\infty + C_1^T C_1 = 0 \tag{2-12}$$

$$\hat{X} A^T + A\hat{X} + (\gamma^{-2} B_1 B_1^T - B_2 B_2^T) + \hat{X} C_1^T C_1 \hat{X} = 0. \tag{2-13}$$

In the beginning of the section, we assumed that $(C_1, -A)$ is detectable. In this case, it is easy to see that $X_\infty(\gamma) = \hat{X}^{-1}(\gamma)$ almost everywhere on $(\alpha_x, +\infty)$ and $X_\infty(\gamma) > 0$ on $(\beta_x, +\infty)$. This assumption will be removed in the following.

In the case that $(C_1, -A)$ is not detectable, one can always find an orthogonal matrix

$$U = [\, U_1 \quad U_2 \,] \tag{2-14}$$

such that

$$U^T A U = \begin{bmatrix} U_1^T A U_1 & 0 \\ U_2^T A U_1 & U_2^T A U_2 \end{bmatrix}, \tag{2-15}$$

$$U^T B = [U^T B_1 \quad U^T B_2] = \begin{bmatrix} U_1^T B_1 & U_1^T B_2 \\ U_2^T B_1 & U_2^T B_2 \end{bmatrix} \tag{2-16}$$

and

$$C_1 U = [C_1 U_1 \quad 0] \tag{2-17}$$

with $(C_1 U_1, -U_1^T A U_1)$ detectable [27]. Furthermore, the solution to (2-12) can be expressed as

$$X_\infty(\gamma) = U \begin{bmatrix} X(\gamma) & 0 \\ 0 & 0 \end{bmatrix} U^T \tag{2-18}$$

with $X(\gamma) = \hat{X}^{-1}(\gamma)$ almost everywhere on $(\alpha_x, +\infty)$, where $X(\gamma)$ and $\hat{X}(\gamma)$ are the stabilizing solutions to (2-12) and (2-13) respectively with (A, B_1, B_2, C_1) replaced by $(U_1^T A U_1, U_1^T B_1, U_1^T B_2, C_1 U_1)$. Therefore, no matter whether $(C_1, -A)$ is detectable or not, it is always true that $X_\infty(\gamma)$ exists almost everywhere on $(\alpha_x, +\infty)$ and $X_\infty(\gamma) \geq 0$ on $(\beta_x, +\infty)$. Moreover, we have the following theorem which gives the properties of the first and second derivatives of $X_\infty(\gamma)$.

Theorem 2.3: On $(\beta_x, +\infty)$,

a) $$\dot{X}_\infty(\gamma) := \frac{d}{d\gamma}(X_\infty(\gamma)) \leq 0, \tag{2-19}$$

b) $$\ddot{X}_\infty(\gamma) := \frac{d^2}{d\gamma^2}(X_\infty(\gamma)) \geq 0. \tag{2-20}$$

Again, next theorem gives the eigen properties for $X_\infty(\gamma)$.

Theorem 2.4: On $(\beta_x, +\infty)$,

a) all eigenvalues of $X_\infty(\gamma)$ are smooth, nonincreasing functions of γ;

b) the maximal eigenvalue of $X_\infty(\gamma)$ is a nonincreasing, convex function of γ.

Similarly, we can obtain the same results for $Y_\infty(\gamma)$, the stabilizing solution to

$$Y_\infty A^T + A Y_\infty + Y_\infty(\gamma^{-2} C_1^T C_1 - C_2^T C_2) Y_\infty + B_1 B_1^T = 0. \tag{2-21}$$

If $(-A, B_1)$ is stabilizable, then $Y_\infty(\gamma)= \hat{Y}^{-1}(\gamma)$ almost everywhere on $(\alpha_y, +\infty)$ and $Y_\infty(\gamma)> 0$ on $(\beta_y, +\infty)$, where $\hat{Y}(\gamma)$ is the stabilizing solution to

$$A^T\hat{Y} + \hat{Y}A + (\gamma^{-2}C_1^TC_1 - C_2^TC_2)+\hat{Y}B_1B_1^T\hat{Y} = 0 \tag{2-22}$$

and

$$\alpha_y := \inf \{\gamma : \gamma\in \mathbb{R}_+ \text{ and } Y_\infty(\gamma) \text{ exists}\} \tag{2-23}$$

$$\beta_y := \inf \{\gamma : \gamma\in \mathbb{R}_+ \text{ and } Y_\infty(\gamma) \text{ is positive semidefinite}\}. \tag{2-24}$$

If $(-A, B_1)$ is not stabilizable, then an orthogonal matrix $V= [V_1 \;\; V_2]$ can be found such that

$$V^TAV=\begin{bmatrix} V_1^TAV_1 & V_1AV_2 \\ 0 & V_2^TAV_2 \end{bmatrix},\; V^TB_1=\begin{bmatrix} V_1^TB_1 \\ 0 \end{bmatrix} \text{ and } CV =\begin{bmatrix} C_1V \\ C_2V \end{bmatrix}=\begin{bmatrix} C_1V_1 & C_1V_2 \\ C_2V_1 & C_2V_2 \end{bmatrix}$$

with $(-V_1^TAV_1,\; V_1^TB_1)$ stabilizable. Furthermore, the stabilizing solution to (2.21) can be expressed as

$$Y_\infty(\gamma) = V\begin{bmatrix} Y(\gamma) & 0 \\ 0 & 0 \end{bmatrix}V^T, \tag{2-25}$$

with $Y(\gamma)= \hat{Y}^{-1}(\gamma)$ almost everywhere on (α_y, ∞) and $Y(\gamma)> 0$ on $(\beta_y, +\infty)$. Again, $Y(\gamma)$ and $\hat{Y}(\gamma)$ are the stabilizing solutions to (2-21) and (2-22) respectively with (A, B_1, C_1, C_2) replaced by $(V_1^TAV_1,\; V_1^TB_1,\; C_1V_1,\; C_2V_1)$. Note that all results presented above for $X_\infty(\gamma)$, $X(\gamma)$ and $\hat{X}(\gamma)$ have their counterparts for $Y_\infty(\gamma)$, $Y(\gamma)$ and $\hat{Y}(\gamma)$ respectively.

Before moving to the next theorem to investigate the properties of $X_\infty Y_\infty$, we define α and β as follows:

$$\alpha := \max\{\alpha_x,\; \alpha_y\} \tag{2-26}$$

$$\beta := \max\{\beta_x,\; \beta_y\}. \tag{2-27}$$

With these definitions, we can see that $X_\infty Y_\infty$ exists on $(\alpha, +\infty)$ almost everywhere. Moreover, $X_\infty Y_\infty$ has no negative eigenvalues on $(\beta, +\infty)$, since both X_∞ and Y_∞ are positive semidefinite on $(\beta, +\infty)$. Now, we are in the position to state our main result.

Theorem 2.5: On $(\beta, +\infty)$,

a) all eigenvalues of $X_\infty Y_\infty$ are smooth, nonincreasing functions of γ;

b) $\rho(X_\infty Y_\infty)$ is a nonincreasing, convex function of γ.

Furthermore, if we define $\rho(\gamma) := \rho(X_\infty Y_\infty)$ and $\dot{\rho}(\gamma) := \frac{d(\rho(\gamma))}{d\gamma}$ on $(\beta, +\infty)$, the slope of $\rho(\gamma)$ can be expressed as

$$\dot{\rho}(\gamma) = \frac{v^T(\dot{X}_\infty Y_\infty + X_\infty \dot{Y}_\infty)w}{v^T w}, \tag{2-28}$$

where v and w are the left and the right eigenvectors of $X_\infty Y_\infty$ respectively corresponding to its maximal eigenvalue. $\dot{X}_\infty$ and $\dot{Y}_\infty$ can be obtained by solving the following Lyapunov equations:

$$\hat{A}^T\dot{X}_\infty + \dot{X}_\infty\hat{A} - 2\gamma^{-3}X_\infty B_1 B_1^T X_\infty = 0 \tag{2-29}$$

and

$$\tilde{A}\dot{Y}_\infty + \dot{Y}_\infty\tilde{A}^T - 2\gamma^{-3}Y_\infty C_1^T C_1 Y_\infty = 0, \tag{2-30}$$

with $\hat{A} = A + (\gamma^{-2}B_1B_1^T - B_2B_2^T)X_\infty$ and $\tilde{A} = A + Y_\infty(\gamma^{-2}C_1^TC_1 - C_2^TC_2)$.

2.2 ALGORITHMS TO COMPUTE THE OPTIMAL H^∞ NORM

According to DGKF theorem, we can see that finding the optimal H_∞ norm, denoted as γ_∞, is equivalent to finding the infimum γ such that all three conditions in (2-5) hold. From the previous subsection, it is obvious that $\gamma_\infty \in [\beta, +\infty)$. It is possible for β to be γ_∞, especially when β and α are identical, however, with very few exceptions, $\gamma_\infty \in (\beta, +\infty)$, which implies that γ_∞ is the solution to $\rho(\gamma) = \gamma^2$. The relations between α, β and γ_∞ are shown in the figure below.

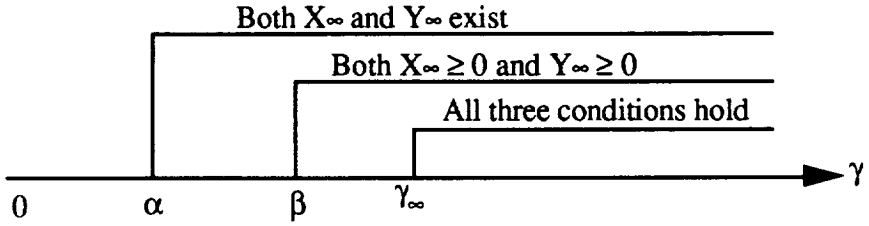

Fig. 2.1

The figure implies that the problem of finding the optimal γ_∞ is actually that of either searching for the intersection point of $\rho(\gamma)$ with γ^2 inside $(\beta, +\infty)$ or computing the boundary point β. Since $\rho(\gamma)$ is a convex function on $(\beta, +\infty)$, then gradient searching method can be employed.

Assume that we have a starting point γ_n in the interval (β, γ_∞), then the optimal γ can be obtained easily as follows. Refer to Fig. 2.2, draw the tangent line with slope $\dot{\rho}(\gamma_n)$

passing through the point $(\gamma_n, \rho(\gamma_n))$. The abscissa, γ_{n+1}, of the intersection of the tangent line and the curve $y = \gamma^2$, always lies between γ_n and γ_∞. The search process is repeated until the gap $\gamma_\infty - \gamma_{n+1}$ is small enough.

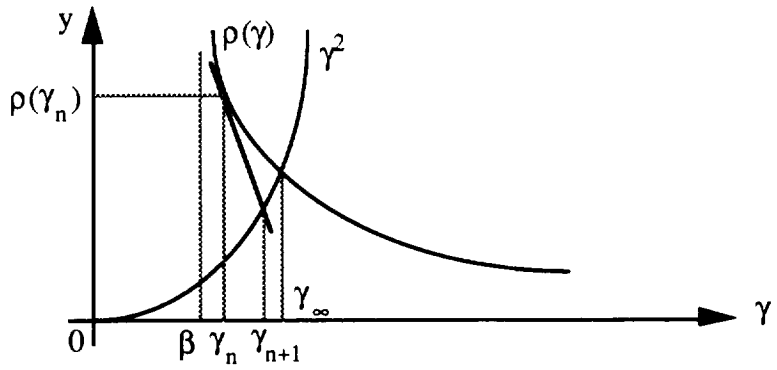

Fig. 2.2

Furthermore, we will see that the convergence rate is quadratic. Define $\varepsilon_n = \gamma_\infty - \gamma_n$ and $\varepsilon_{n+1} = \gamma_\infty - \gamma_{n+1}$. It is straightforward to show that

$$\varepsilon_{n+1} \approx \frac{\ddot{\rho}(\gamma_\infty)}{2 \mid \dot{\rho}(\gamma_\infty) - 2\gamma_\infty \mid} \varepsilon_n^2 \qquad (2\text{-}31)$$

which implies quadratic convergence. For convenience, the algorithm described will be referred to as **Q-step**, since the quadratic convergence is guaranteed, provided there is a starting point $\gamma_n \in (\beta, \gamma_\infty)$ to start with.

Based on the discussion above, following procedure is given to compute the optimal H_∞ norm.

Step 1. Initial point

Refer to Fig. 2.1, choose a relatively large initial γ_1 such that $\gamma_1 \in [\beta, +\infty)$. If $\gamma_1 \in (\beta, \gamma_\infty)$, then it can be used as the starting point for γ_∞. Go to Q-step. If $\gamma_1 \in (\gamma_\infty, +\infty)$, which implies $X_\infty(\gamma_1) \geq 0$ and $Y_\infty(\gamma_1) \geq 0$, then go to step 2.

Step 2. Starting point for γ_∞

Evaluate $\rho(\gamma)$ at γ_1, we have the point $(\gamma_1, \rho(\gamma_1))$. Refer to Fig. 2.3, draw a line passing through the point $(\gamma_1, \rho(\gamma_1))$ with slope $\dot{\rho}(\gamma_1)$. The abscissa, γ_2, of the intersection of the straight line and the curve $y = \gamma^2$, is always less than γ_∞. If $\gamma_2 \in (\beta, \gamma_\infty)$, then we are ready to go to Q-step with γ_2 as the starting point γ_n in Fig. 2.2.

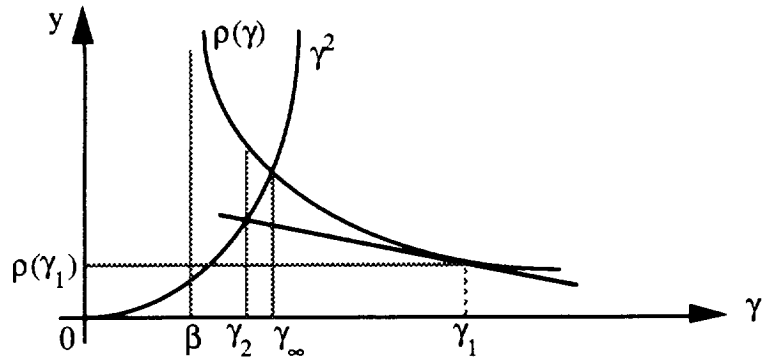

Fig. 2.3

Remark: Most of the time, the method described in the previous paragraph gives the starting point γ_n inside the interval (β, γ_∞). However, this method may fail, see Fig. 2.4 and Fig. 2.5. For the case described by Fig. 2.4, a smaller γ_1 could do the job. However, for the case of Fig. 2.5, γ_2 is always less than α, and therefore less than β, no matter how small γ_1 is. Since it is difficult to tell which case we are facing and there is no efficient guideline to reduce γ_1, we suggest to continue if two or three rials of γ_1 does not give a starting point.

If $\gamma_2 \in (\alpha, \beta)$, go to step 3 to compute β. If $\gamma_2 < \alpha$, then go to step 4 to compute α.

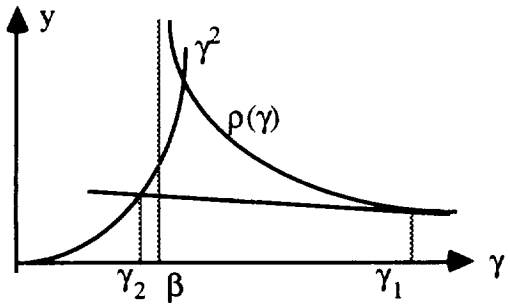

Fig. 2.4

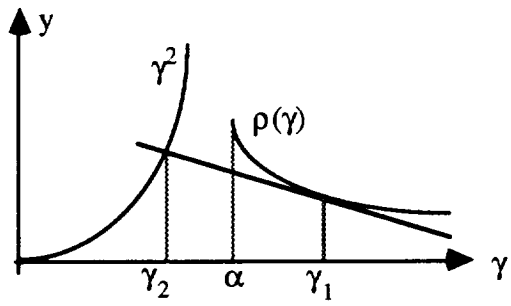

Fig. 2.5

Step 3. Computing β

For the computation of β, one also needs a starting point to use Newton method. It is similar to the gradient method described earlier. See Appendix for details. Note that the γ_2 obtained in step 2 can be used as a starting point for β. If β is optimal γ (i.e., all the three conditions in (2-5) are satisfied), see Fig. 2.1, then the algorithm will terminate here. Otherwise $\beta+\varepsilon$ can be served as the starting point γ_n for γ_∞ in Fig. 2.2, where ε is a very small positive real number. Go to Q-step.

Step 4. Computing α

If either $X_\infty(\gamma_2)$ or $Y_\infty(\gamma_2)$ does not exist, which implies $\gamma_2 < \alpha$, we will compute α first. Appendix will give the algorithm for the computation of α. If α is optimal γ (i.e.,

all the three conditions in (2-5) are satisfied), see Fig. 2.1, then the algorithm will terminate here. Otherwise α can be used either as a starting point for β, when $\alpha \neq \beta$; or a starting point for γ_∞, when $\alpha = \beta$. Go to step 3 and Q-step respectively.

Q-step. Computing γ_∞

This step was described in Fig. 2.2. We can see from the earlier discussion, once we have a starting point for γ_∞, the quadratic convergence is guaranteed. Algorithm terminates.

Example 2.1: The following is a simple H^∞ optimization problem which is used to illustrate the proposed algorithm of computing the optimal H^∞ norm. A realization of the generalized plant G(s) is given by

$$G(s) = \left[\begin{array}{c|cc} A & B_1 & B_2 \\ \hline C_1 & D_{11} & D_{12} \\ C_2 & D_{21} & D_{22} \end{array}\right] = \left[\begin{array}{cc|cc|c} -1 & 0 & 1 & 0 & 0 \\ 0 & 2 & 0 & 0 & 1 \\ \hline 1 & 1 & 0 & 0 & 0 \\ 0 & 0 & 0 & 0 & 1 \\ \hline 1 & 1 & 0 & 1 & 0 \end{array}\right].$$

Starting from $\gamma_0 = 100$, we have $\rho(\gamma_0) = \rho[X_\infty(\gamma_0)Y_\infty(\gamma_0)] = 2.16e01$. The slope of $\rho(\gamma)$ at this point $(\gamma_0, \rho(\gamma_0))$ is $\dot{\rho}(\gamma_0) = -3.49e\text{-}05$. The tangent line at this point will intersect with the curve $y = \gamma^2$ at $\gamma_1 = 4.65$. Again, evaluate $\rho(\gamma_1) = 2.24e01$ and compute the slope $\dot{\rho}(\gamma)$ at $(\gamma_1, \rho(\gamma_1))$. Since $\rho(\gamma_1) > \gamma_1^2$, γ_1 is inside the interval (β, γ_∞) and therefore from now on the convergence is guaranteed. The process is repeated until the gap between $\sqrt{\rho(\gamma_n)}$ and γ_n is small enough. The following data show that only four iterations are needed to reach the optimum, $\gamma_{op} = 4.734160476390407$, with accuracy better than 10^{-14}.

Iter	γ_n	$\lvert\sqrt{\rho(\gamma_n)} - \gamma_n\rvert$	$\dot{\rho}(\gamma_n)$
0	100	9.535e+01	-3.487e-05
1	4.647998761538930e+00	8.403e-01	-3.811e-01
2	4.734064423866624e+00	9.440e-04	-3.595e-01
3	4.734160476276923e+00	1.115e-09	-3.595e-01
4	4.734160476390407e+00	7.105e-15	

By the formulas in (2-6) and the descriptor-form technique described in [26], we are able to construct an optimal controller as follows:

$$K_{opt}(s) = \left[\begin{array}{c|c} -.87542 & -0.13925 \\ \hline 4.42042 & -4.73416 \end{array}\right]$$

with the H^∞ norm of the closed-loop system equals γ_{op}. Note that the optimal controller has a direct feedthrough term and thus has infinite bandwidth. If we choose $\gamma = 4.8$ which is about 1.4% higher than γ_{op}, we have a suboptimal controller

$$K_{opt}(s) = \left[\begin{array}{cc|c} -8.67072e\text{-}01 & 1.32928e\text{-}01 & -1.38959e\text{-}01 \\ -1.38320e{+}01 & -1.52323e{+}02 & 4.73733e{+}00 \\ \hline -9.30025e{+}00 & -1.49792e{+}02 & 0 \end{array}\right]$$

which has a reasonable bandwidth and the closed-loop H^∞ norm, $\|T_{zv}\|_\infty < 4.8$ which is only 1.4% away from the optimal H^∞ norm.

2.3 Formulation of H^∞ Optimization Problems

Many control problems can be formulated as the standard H^∞ optimization problem. For the purpose of demonstration, two examples are given in the following. The first is a mixed-sensitivity optimization problem to be formulated as a two-block H^∞ optimization problem; the second is a disturbance reduction problem with measurement noise which turns out to be a four-block problem.

A. Mixed-Sensitivity Optimization Problem

Consider the following system:

$$y(s) = P(s)u(s) + v(s) \qquad (2\text{-}32a)$$

$$u(s) = K(s)y(s) \qquad (2\text{-}32b)$$

where v(s) is disturbance, y(s) is output and K(s) is controller to be designed. It is well known that a smaller $\|(I-PK)^{-1}\|_\infty$ means a better disturbance attenuation, whereas a smaller $\|PK(I-PK)^{-1}\|_\infty$ implies a better robust stability. Unfortunately, the H^∞ norms of $(I-PK)^{-1}$ and $PK(I-PK)^{-1}$ may not be made small at the same time. If we make one of them smaller then the other will become larger. To have a trade-off between these two quantities, Kwakernaak [24] formulated the mixed-sensitivity problem as the problem of finding a controller K(s) which stabilizes the closed-loop system and minimizes $\|\Phi\|_\infty$ where Φ is given by

$$\Phi = \begin{bmatrix} W_1(I-PK)^{-1} \\ W_2PK(I-PK)^{-1} \end{bmatrix} \tag{2-33}$$

W_1 and W_2 are weighting matrices chosen by the designer according to the concrete situation. In other words, they depend on the characters of the disturbances and system uncertainties. Usually, the disturbances occur most likely at low frequency, therefore $W_1(s)$ is chosen to be a low-pass filter to emphasize the error energy at low frequency. The plant uncertainty is also frequency-dependent; the higher the frequency is, the larger the uncertainties become. Hence, $W_2(s)$ is usually chosen to be a improper transfer function (but $W_2P(s)$ has to be a proper transfer function), which is analytic in closed right half plane. In the following, we assume that $W_1(s)$ is strictly proper, $W_2(s)$ is a polynomial such that $W_2P(s)$ remains proper and both of them are analytic in closed right half plane.

The problem of finding a K(s) which stabilizes the closed-loop system and minimizes $\|\Phi\|_\infty$ can be rearranged into the standard H^∞ optimization problem. Consider the following system:

$$\begin{bmatrix} z_1 \\ z_2 \\ y \end{bmatrix} = \left[\begin{array}{c|c} W_1 & W_1P \\ 0 & W_2P \\ \hline I & P \end{array}\right] \begin{bmatrix} v \\ u \end{bmatrix} \tag{2-34a}$$

$$u = K\,y \tag{2-34b}$$

It is easy to show that the matrix Φ defined by (2-33) is just the transfer function from v to $[z_1^T \; z_2^T]^T$ of the closed-loop system (2-34). Comparing (2-34a) with (2-1a), we can see that

$$G_{11} = \begin{bmatrix} W_1 \\ 0 \end{bmatrix}, \qquad G_{12} = \begin{bmatrix} W_1P \\ W_2P \end{bmatrix},$$
$$G_{21} = I, \qquad G_{22} = P. \tag{2-35}$$

If P, W_2P, and W_1 have state-space realizations as follows

$$P = \left[\begin{array}{c|c} A_p & B_p \\ \hline C_p & D_p \end{array}\right], \; W_2P = \left[\begin{array}{c|c} A_p & B_p \\ \hline C_{w2} & D_{w2} \end{array}\right], \; W_1 = \left[\begin{array}{c|c} A_{w1} & B_{w1} \\ \hline C_{w1} & D_{w1} \end{array}\right] \tag{2-36}$$

Then the generalized plant G(s) has a state space realization as shown in (2-2) with

$$A = \begin{bmatrix} A_p & 0 \\ B_{w1}C_p & A_{w1} \end{bmatrix}, \quad B_1 = \begin{bmatrix} 0 \\ B_{w1} \end{bmatrix}, \quad B_2 = \begin{bmatrix} B_p \\ B_{w1}D_p \end{bmatrix}$$

$$C_1 = \begin{bmatrix} D_{w1}C_p & C_{w1} \\ C_{w2} & 0 \end{bmatrix}, \quad D_{11} = \begin{bmatrix} D_{w1} \\ 0 \end{bmatrix}, \quad D_{12} = \begin{bmatrix} D_{w1}D_p \\ D_{w2} \end{bmatrix}$$

$$C_2 = [C_p \quad 0], \qquad D_{21} = I, \qquad D_{22} = D_p \tag{2-37}$$

Note that because W_2 is a polynomial, the A-matrix of W_2P is same as that of P.

B. Disturbance Reduction Problem

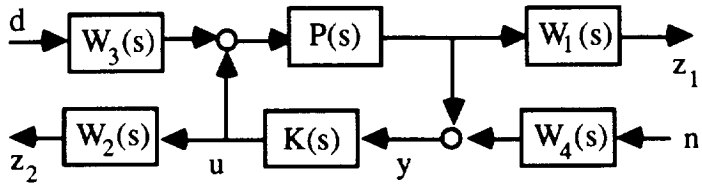

Fig.2.6 A disturbance attenuation problem

Consider the feedback system shown in Fig.2.6. P(s) is a given plant, $W_i(s)$, i=1,2,3,4 are weighting matrices, and K(s) is the controller to be designed. The disturbance and noise are the outputs of W_3 and W_4 driven by d and n respectively. z_1 is the weighted error response; z_2 is the weighted control input. Let $z^T = [z_1^T \; z_2^T]^T$, $v^T = [d^T \; n^T]^T$ and assume that v is unknown but with its energy bounded by unity. The objective is to find a controller K(s) which stabilizes the closed-loop system and minimizes the worst $\|z\|_2$, i.e., minimizes the H^∞ norm of T_{zv}, the closed-loop transfer function from v to z. T_{zv} is given by

$$T_{zv} = \begin{bmatrix} W_1P(I-KP)^{-1}W_3 & W_1PK(I-PK)^{-1}W_4 \\ W_2KP(I-KP)^{-1}W_3 & W_2K(I-PK)^{-1}W_4 \end{bmatrix} \tag{2-38}$$

Note that $W_1PK(I-PK)^{-1}W_4$ and $W_2KP(I-KP)^{-1}W_3$) are the output and input complementary sensitivity functions. Their H^∞ norms indicate the stability robustness of the closed-loop system for the multiplicative plant uncertainty introduced at the output and input respectively. $W_2K(I-PK)^{-1}W_4$ is the control complementary sensitivity function whose H^∞ norm indicates the stability robustness of the closed-loop system for additive plant uncertainty. Hence, reducing $\|T_{zv}\|_\infty$ will also improve the robust stability of the closed-loop system.

It is easy to verify that the generalized plant of the system can be expressed as:

$$\begin{bmatrix} z_1 \\ z_2 \\ \hline y \end{bmatrix} = \left[\begin{array}{cc|c} W_1PW_3 & 0 & W_1P \\ 0 & 0 & W_2 \\ \hline PW_3 & W_4 & P \end{array}\right] \begin{bmatrix} d \\ n \\ \hline u \end{bmatrix} \tag{2-39}$$

That is,

$$G_{11} = \begin{bmatrix} W_1PW_3 & 0 \\ 0 & 0 \end{bmatrix}, \quad G_{12} = \begin{bmatrix} W_1P \\ W_2 \end{bmatrix}$$
$$G_{21} = \begin{bmatrix} PW_3 & W_4 \end{bmatrix}, \quad G_{22} = P. \tag{2-40}$$

If P, W_i, i=1,2,3,4 have state-space realizations as follows:

$$P = \left[\begin{array}{c|c} A_p & B_p \\ \hline C_p & D_p \end{array}\right], \quad W_i = \left[\begin{array}{c|c} A_{wi} & B_{wi} \\ \hline C_{wi} & D_{wi} \end{array}\right], \quad i=1,2,3,4 \tag{2-41}$$

Then the generalized plant G(s) has a state space realization as shown in (2-2) with

$$A = \begin{bmatrix} A_p & 0 & 0 & B_pC_{w3} & 0 \\ B_{w1}C_p & A_{w1} & 0 & B_{w1}D_pC_{w3} & 0 \\ 0 & 0 & A_{w2} & 0 & 0 \\ 0 & 0 & 0 & A_{w3} & 0 \\ 0 & 0 & 0 & 0 & A_{w4} \end{bmatrix}, \quad B_1 = \begin{bmatrix} B_pD_{w3} & 0 \\ B_{w1}D_pD_{w3} & 0 \\ 0 & 0 \\ B_{w3} & 0 \\ 0 & B_{w4} \end{bmatrix}, \quad B_2 = \begin{bmatrix} B_p \\ B_{w1}D_p \\ B_{w2} \\ 0 \\ 0 \end{bmatrix}$$

$$C_1 = \begin{bmatrix} D_{w1}C_p & C_{w1} & 0 & D_{w1}D_pC_{w3} & 0 \\ 0 & 0 & C_{w2} & 0 & 0 \end{bmatrix}, \quad D_{11} = \begin{bmatrix} D_{w1}D_pD_{w3} & 0 \\ 0 & 0 \end{bmatrix}, \quad D_{12} = \begin{bmatrix} D_{w1}D_p \\ D_{w2} \end{bmatrix}$$

$$C_2 = \begin{bmatrix} C_p & 0 & 0 & D_pC_{w3} & C_{w4} \end{bmatrix}, \quad D_{21} = \begin{bmatrix} D_pD_{w3} & D_{w4} \end{bmatrix}, \quad D_{22} = D_p\,. \tag{2-42}$$

Above {A,B,C,D} is the state-space representation for the generalized plant G(s).

2.4 A Design Approach to Achieve H^2/H^∞ Objectives

The mixed H^2 and H^∞ control problem in its most general form has not been solved as of yet. However, taking advantage of the recent advances in H^∞ theory, we believe that it is possible to develop a simple design procedure that will address the performance-

robustness problem. In the following, we consider the disturbance attenuation problem with control weighting as shown in Figure 2.6. The nominal plant is denoted by $\mathcal{P}(s)$ and the energy bounded exogenous signals consist of plant input disturbances d and measurement noise n. The weighted error response and the weighted control input consist of z_1 and z_2, respectively.

Following the approach presented by Doyle et. al. in [1,2], this problem can easily be transformed to the general H^2/H^∞ configuration. The task is then to design a stabilizing H^∞ controller K(s) such that the H^∞ norm of the transfer function matrix from the exogenous input vector $w^T = [\, d^T \;\; n^T \,]^T$ to the output vector $z^T = [\, z_1^T \;\; z_2^T]^T$ is minimized. From Figure 2.6, this transfer function matrix is given by:

$$T_{zw} = \begin{bmatrix} W_1 P (I - K P)^{-1} W_3 & W_1 P K (I - P K)^{-1} W_4 \\ W_2 K P (I - K P)^{-1} W_3 & W_2 K (I - P K)^{-1} W_4 \end{bmatrix} \qquad (2\text{-}43)$$

where W_i (s), i = 1, ... ,4 are weights to be chosen by the designer appropriate to the plant and design objectives being considered. Usually, W_3 is a low frequency filter indicating that the disturbances introduced at the plant input are low frequency signals. The rest are usually assumed to be high frequency filters to include measurement noise, unmodeled dynamics, and any other plant uncertainties that may occur at high frequencies. Notice that W_1 can be nonproper, hence providing the flexibility to consider frequency dependent output responses. In this note however, we will only consider weights that lead to controllers having the same order as that of the nominal plant.

The above disturbance rejection problem turns out to be a four-block problem and its solution is described in [2]. It has been realized however, that suboptimal controller, i.e. controllers satisfying $\| T_{zw} \|_\infty < \gamma$ for some positive γ greater than the optimal H^∞-norm of the closed-loop transfer matrix, are much easier to characterize than optimal ones. It also turns out that the variable γ can be used as a design parameter. This can easily be verified when the general mixed H^2/H^∞ control problem is restricted to the case where the H^2 closed-loop transfer matrix is the same as that of the H^∞ problem. In this case, the suboptimal H^∞ controller approaches the H^2/LQG controller as γ approaches ∞.

From the input/output relation described above, it can be seen that it is possible to address the performance/robustness problem via the design weights. For instance, the complementary sensitivity function which is a measure of the closed-loop robustness is represented by the (1,2) block of the closed-loop transfer matrix above with the weights W_1 and W_4 included. Thus by appropriately choosing these weights one can hope to gain on performance without giving up too much robustness. As we will see later in the

example, this procedure when used effectively is comparable to the LTR technique as far as H^2 performance and robustness are concerned.

Example 2.2

Consider the following typical LQG problem:

$$\dot{x} = \begin{bmatrix} 0 & 1 \\ -3 & -4 \end{bmatrix} x + \begin{bmatrix} 0 \\ 1 \end{bmatrix} u + \begin{bmatrix} 35 \\ -61 \end{bmatrix} d$$

$$y = [\, 2 \quad 1 \,]\, x + n$$

with $E(d) = E(n) = 0$; $E[d(t)d(\tau)] = E[n(t)n(\tau)] = \delta(t-\tau)$. The following performance index is of particular interest

$$J = \int_0^\infty (x^T Q^T Q\, x + u^2)\, dt \quad \text{where} \quad Q = 4\sqrt{5}\,[\sqrt{35} \quad 1\,]$$

In the H^∞ formulation, we construct the generalized plant

$$G(s) = \left[\begin{array}{c|cc} A & B_1 & B_2 \\ \hline C_1 & D_{11} & D_{12} \\ C_2 & D_{21} & D_{22} \end{array}\right]$$

by considering the same nominal plant as in the LQG problem with the following weights:

$W_1(s) = \alpha_1 \dfrac{s^2 + 10\,s + 4}{s + 2}$ and $W_{2,3,4}(s) = \alpha_{2,3,4}$ where the αi's are real. The optimal LQG performance index turns out to be equal to 493. Introducing a fictitious noise at the plant input as described by the LTR technique improves the stability margins of the closed-loop system, but at the expense of performance. The solid-line curve 3 in Figure 2.7 represents the singular values of the complementary sensitivity function with the LQG controller implemented while curve 4 corresponds to the LTR design. The improvement in robustness using the LTR technique results in a loss in performance as summarized in the table below. The dashed line Curve 1 in Figure 2.7 corresponds to the implementation of the (α-design) H^∞ controller with the constants $\alpha_1 = \alpha_2 = \alpha_3 = 1$ and $\alpha_4 = 0.01$. The reason why α_4 was varied was because it is directly related to the complementary sensitivity function as indicated by the input-output relations above. The suboptimal H^∞ controller was obtained for a value of γ that is 15% higher than the optimal H^∞ norm.

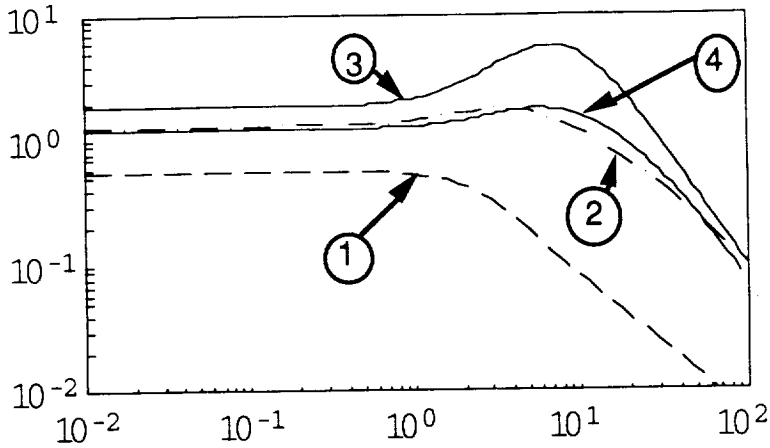

Figure 2.7 Complementary sensitivity function (db)

Curve 2 corresponds to the implementation of a H^∞ controller (β-design) with the following data:

$$B_1 = \beta_1 \begin{bmatrix} 35 & 0 \\ -61 & 0 \end{bmatrix} \quad C_1 = \beta_2 \begin{bmatrix} 20\sqrt{7} & 4\sqrt{5} \\ 0 & 0 \end{bmatrix}$$

$$D_{12} = \beta_3 \begin{bmatrix} 0 \\ 1 \end{bmatrix} \qquad D_{21} = \beta_4 [\, 0 \quad 1]$$

Notice that the case when all the constants β_i's equal to 1 corresponds to the special case of the mixed H^2/H^∞ control where both the H^2 and H^∞ closed-loop transfer matrices are the same. Curve 2 which was obtained by setting β_2 and β_4 to be equal to 0.1. Notice that at high frequencies curve 2 is below curve 4 (LQG/LTR) indicating a better robustness measure. The resulting performance index in this case is the same as the LTR case, i.e. equal to 587. One interesting point can be seen in here by examining the open-loop Nyquist plots of the LQG/LTR controller and the H^∞ controller shown in Figure 2.8. The dashed-line curve which corresponds to the H^∞ controller implementation illustrates a phase margin that is almost 10 degrees better than that of the LTR design. There is however a loss of 1 db in gain margin. It is not clear exactly why this happens but we intend to look into the problem in further research.

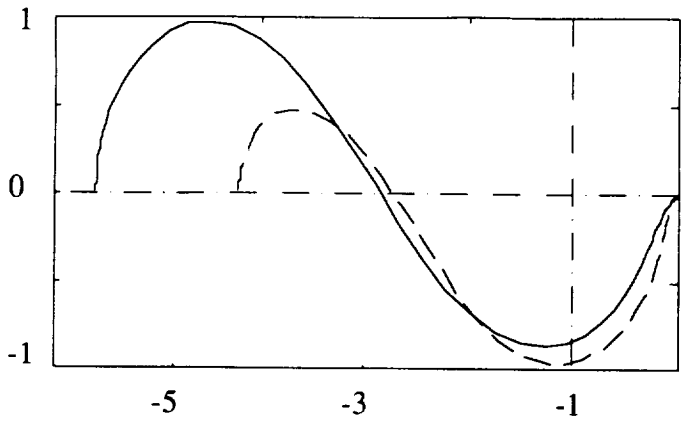

Figure 2.8. Nyquist Plots

2.5 Computation of the Real Structured Singular Value

For a large class of linear time-invariant systems with real parametric perturbations, the coefficient vector of the characteristic polynomial is a multilinear function of the real parameter vector. Based on this multilinear mapping together with the recent results by De Gaston and Safonov [15], Sideris and Pena [16], Bartlett, Hollot, and Lin [18], and Bouguerra, Chang, Yeh, and Banda [23], an algorithm for computing the real structured singular value is proposed. The algorithm requires neither frequency search nor Routh's array symbolic manipulations and allows the dependency among the elements of the parameter vector. Moreover, the number of the independent parameters in the parameter vector is not limited to three, as is required by many existing structured singular value computation algorithms.

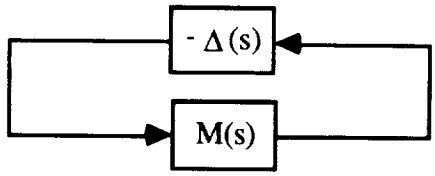

Fig.2.9 Standard structure for a perturbed closed-loop system.

All the plant uncertainties, structured or unstructured, unmodeled dynamics or parametric perturbations, can be described by the block diagram shown in Fig.2.9. In Fig.2.9, $\Delta(s)$ = block diag { $\Delta_1(s)$, $\Delta_2(s)$, ..., $\Delta_m(s)$ } and M(s) is the nominal system which includes the nominal plant and the stabilizing controller. The structured singular value (SSV) is defined based on the above perturbation structure. The SSV is nonconservative scalar stability-margin measures for multivariable systems.

Algorithms [6,7] to compute the SSV are available only for those cases where the number of perturbation blocks are less than or equal to three. The computational problem

for the cases with more than three perturbation blocks is still an unsolved problem.

One important special case of plant uncertainties is the real parametric perturbation. In this case the perturbation matrix $\Delta(s)$ is a real diagonal matrix. The SSV defined for this case is called the real SSV. An iterative algorithm of computing the real SSV for real diagonal Δ was developed by De Gaston and Safonov [15] and generalized by Pena and Sideris [16]. There is no limitation on the number of perturbation parameters. However, this iterative algorithm is complicated since an extensive frequency search is required.

In the following we assume that the perturbation matrix Δ in Fig.2.9 is real diagonal, i.e., $\Delta = \text{diag}\ \{ \bar{\delta}_1, \bar{\delta}_2, \ ..., \ \bar{\delta}_m \}$ and the nominal system M(s) is a rational matrix with real coefficients. If the parameters vary independently and $-1 \le \bar{\delta}_i \le 1$, $i = 1,2,...,m$, the parameter perturbation domain $\mathfrak{D}$ can be described as a hyper-cube $\bar{\mathfrak{D}}$ with 2^m vertices $(\pm 1, ..., \pm 1)$ in the m-dimensional real space. In general, the perturbation matrix Δ can be written as $\Delta = \text{diag}\ \{\delta_1 I_{m1}, \delta_2 I_{m2}, ..., \delta_r I_{mr}\}$ where I_{mi} is the identity matrix of order mi and $m1+m2+ ...+mr = m$. That is, $\bar{\delta}_1 = \bar{\delta}_2 = \cdots = \bar{\delta}_{m1} = \delta_1$, $\bar{\delta}_{m1+1} = \bar{\delta}_{m1+2} = \cdots = \bar{\delta}_{m1+m2} = \delta_2$, ..., etc. In this case, the parameter perturbation domain $\mathfrak{D}$ is an r-dimensional hyperplane inside the m-dimensional hypercube $\bar{\mathfrak{D}}$. The system is said to be <u>robustly stable in $\mathfrak{D}$</u> if and only if it is stable for every parameter vector $\bar{\delta} = [\ \bar{\delta}_1 \ \ \bar{\delta}_2 \ \ ... \ \ \bar{\delta}_m\ ]^T$ in $\mathfrak{D}$. Throughout the report, we may use "$\mathfrak{D}$ is stable" to replace "the system is robustly stable in $\mathfrak{D}$" whenever there is no confusion.

The <u>real multivariable stability margin</u> (real MSM) k_M is defined as the largest real constant k such that the closed-loop system remains robustly stable in $k\mathfrak{D}$ where $k\mathfrak{D}$ is the enlarged (or shrunk) parameter perturbation domain of $\mathfrak{D}$, i.e.,

$$k\mathfrak{D} := \{ \bar{\delta} : \bar{\delta} = [\delta_1,..,\delta_1, \delta_2..,\delta_2, ..., \delta_r,..,\delta_r] \in \mathbb{R}^m \text{ and } |\delta_i| \le k,\ i=1,2,...,r \} \qquad (2\text{-}44)$$

The enlarged (or shrunk) hypercube of $\bar{\mathfrak{D}}$, $k\bar{\mathfrak{D}}$ is

$$k\bar{\mathfrak{D}} := \{ \bar{\delta} : \bar{\delta} \in \mathbb{R}^m \text{ and } |\delta_i| \le k,\ i=1,2,...,m \}. \qquad (2\text{-}45)$$

Recall that the real structured singular value (real SSV) μ is defined as

$$\mu := [\ \min \{ k \mid \det [I+M(j\omega)\Delta] = 0 \text{ for some } \omega \text{ and } \Delta \in \mathbf{X}(k) \}\ ]^{-1} \qquad (2\text{-}46)$$

where

$$\mathbf{X}(k) = \{ \Delta \mid \text{diag}\ \{\delta_1 I_{m1}, \delta_2 I_{m2}, ..., \delta_r I_{mr}\} \text{ with } |\delta_i| \le k, \text{ for all } i \} \qquad (2\text{-}47)$$

That is, the real SSV μ is the reciprocal of the smallest k such that the system is unstable in

$k_{\mathcal{D}}$. It is easy to see that the relation between the real SSV μ and the real MSM k_M is

$$\mu = 1 / k_M \tag{2-48}$$

As mentioned earlier, several significant results [17-22] have been obtained in the perturbed-characteristic-polynomials approach. Probably the most famous are the Kharitonov's theorems [17] which apply to the special case with a hyper-rectangular perturbed region in the coefficient space. In this special case, the coefficients of the characteristic polynomial vary independently and the robust stability of the system can be easily determined by four bounding characteristic polynomials. Unfortunately, the Kharitonov's theorems cannot be applied to our problem since the coefficient variations of the characteristic polynomial are not independent.

Bartlett, Hollot, and Lin [18] developed an important theorem which is applicable to the case when the coefficients of characteristic polynomial are linearly dependent. The theorem is now well known as the Edge Theorem: For the set of characteristic polynomials inside a polytope $\mathcal{P}$ in the coefficient space, every polynomial in $\mathcal{P}$ is stable if and only if all the exposed edges of $\mathcal{P}$ are stable. This simplifies the stability checking tremendously since checking the stability of exposed edges is much simpler than checking that of the full $\mathcal{P}$. The exposed-edge stability checking is done by sweeping t from 0 to 1 such that

$$t\,\alpha^i + (1-t)\,\alpha^j \tag{2-49}$$

are all stable for all vertices α^i and α^j of $\mathcal{P}$.

Bialas [20] and Fu and Barmish [19] reduced the checking of the exposed-edge sweep stability to a one-shot test. They showed that $t\,\alpha^i + (1-t)\,\alpha^j$ is stable for all $t \in [0,1]$ if and only if the real eigenvalues of $-H_i H_j^{-1}$ are all negative where α^i and α^j are assumed to be stable and H_i and H_j are the Hurwitz matrices for α^i and α^j respectively. Recently, a fast algorithm based on Chapellat and Bhattacharyya's Segment Lemma [22] was proposed by Bouguerra, Chang, Yeh, and Banda [23] for checking the stability of the exposed edges. The computation in the algorithm mainly depends on the number of vertices instead of the edges and therefore reduces the computation burden due to the "combinatoric explosion".

There are no such celebrated properties in the parameter space as those in the coefficient space discovered by Kharitonov [17], Bartlett, Hollot, and Lin [18]. The closed-loop system may be unstable inside $\bar{\mathcal{D}}$ although it is stable at all the edges of the hypercube $\bar{\mathcal{D}}$. So far, there is no easy way of checking robust stability in the parameter space.

For each parameter vector $\bar{\delta}$ in the parameter perturbation domain $\mathcal{D}$, there is a corresponding characteristic polynomial, i.e., a coefficient vector α in the coefficient space. Let $\mathcal{I}(\mathcal{D})$ be the image of $\mathcal{D}$ in the coefficient space. The closed-loop system is robustly stable in $\mathcal{D}$ if and only if every characteristic polynomial in $\mathcal{I}(\mathcal{D})$ is stable. Although several significant results for robust stability have been obtained in the coefficient space, there is no efficient way to check robust stability for $\mathcal{I}(\mathcal{D})$ since $\mathcal{I}(\mathcal{D})$ usually is neither a Kharitonov's hyper-rectangle [17] nor a polytope considered by Bartlett, Hollot, and Lin [18].

Define the polytope $\mathcal{P}(\bar{\mathcal{D}})$ as the convex hull of the 2^m image points in the (n+1)-dimensional coefficient space mapped from the vertices of $\bar{\mathcal{D}}$ where n is the degree of the characteristic polynomial. If the mapping is multilinear then the image of the edges of the hypercube $\bar{\mathcal{D}}$ will be the straight line segments connecting the corresponding mapped vertices. The image of $\mathcal{D}$, $\mathcal{I}(\mathcal{D})$, is a subset of $\mathcal{I}(\bar{\mathcal{D}})$ and therefore is a subset of the polytope $\mathcal{P}(\bar{\mathcal{D}})$. Under the condition of the multilinear mapping, the stability of the edges of $\mathcal{P}(\bar{\mathcal{D}})$ will guarantee the robust stability in $\bar{\mathcal{D}}$. The multilinear mapping can be easily achieved by assuming that the nominal system M(s) in Fig.2.9 is a rational matrix with real coefficients.

Now, we have an easy way to check the sufficient condition for the robust stability in $\mathcal{D}$ by using its corresponding polytope $\mathcal{P}(\bar{\mathcal{D}})$. The sufficient condition is still not enough to determine the real MSM k_M. Any k such that the polytope $\mathcal{P}(k\bar{\mathcal{D}})$ remains stable, say k_L, can be served as a lower bound for k_M. However, there may exist some $k > k_L$ such that $k\mathcal{D}$ is stable although the corresponding polytope $\mathcal{P}(k\bar{\mathcal{D}})$ is unstable.

Any k which cause instability of $k\mathcal{D}$ or $\mathcal{I}(k\mathcal{D})$ qualifies as an upper bound for k_M. To facilitate the description of the relations between the parameter space and the coefficient space, let the edges (vertices, resp.) of $\mathcal{P}(k\bar{\mathcal{D}})$ which are mapped from the edges (vertices, resp.) that are parallel to an axis of coordinates of $k\mathcal{D}$ be called the crucial edges (vertices, resp.) and those which are not crucial be called noncrucial edges (vertices, resp.). The noncrucial edges include two kinds of edges: supplemental edges and fictitious edges. The supplemental edges are the image of the edges of $k\bar{\mathcal{D}}$ which are not in $k\mathcal{D}$. The fictitious edges are the edges of $\mathcal{P}(k\bar{\mathcal{D}})$ which are not mapped from the edges of $k\bar{\mathcal{D}}$. The crucial edges are all in $\mathcal{I}(k\mathcal{D})$. Thus, some k which causes instability at the crucial edges of $\mathcal{P}(k\bar{\mathcal{D}})$, say k_U, may be used as an upper bound for k_M. If the lower and the upper bounds coincide or are close enough, we have the real MSM k_M and the real SSV μ. The objective

of the iterative algorithm to be presented in the paper is to reduce the gap of the lower and the upper bounds. When the gap is smaller than the desired accuracy ε, i.e., $|k_U - k_L| \le \varepsilon$, we have the real MSM $k_M = k_L$ and the real SSV $\mu = 1/k_M$.

2.6. CONTROLLABILITY AND DEGREE OF CONTROLLABILITY

The work performed in controllability has concentrated on discrete-time model representation of linear systems, specifically the deterministic discrete-time system model (sampled data system model) given by:

$$\underline{x}(k+1) = \Phi(k)\,\underline{x}(k) + \Theta(k)\,\underline{u}(k) \quad ; \quad k = k_0, \cdots \tag{2-50}$$

where $\underline{x}(k)$ is the system model state vector representation in R^n at time k

$\underline{u}(k)$ is the system model control vector in R^m at time k

$\Phi(k)$ is the (n-by-n) transition matrix of the system model from the state $\underline{x}(k)$ to $\underline{x}(k+1)$ with zero input applied to the system

$\Theta(k)$ is the (n-by-m) input matrix of the system model at time k

The degree of controllability measures the relation between the input $\underline{u}(k)$ and the state $\underline{x}(k)$ [28]. Recall that the system is ***not*** completely controllable if there exists some direction in state space which ***cannot*** be influenced by a control excitation. Further-more, some directions are more easily influenced than others. Thus, the Degree of Controllability (DOC) of a system must be some measure of the input-to-state gain along the direction in which it is smallest, that is the smallest gain of the input-state map. This gain vanishes if the system is uncontrollable. To define the DOC mathematically , consider the relevant state and input sets for the deterministic linear discrete-time system of Eq.(2-50):

$$\mathbb{X} := \{\, \underline{x}(k) \in \mathbf{R}^n \text{ , for } k_o \ge 0,\ k \in [k_o, k_o+1, k_o+2, \ldots\ldots)\} \quad = \text{set of the states}$$

$$\mathbb{U} := \{\, \underline{u}(k) \in \mathbf{R}^m \text{ , for } k_o \ge 0,\ k \in [k_o, k_o+1, k_o+2, \ldots\ldots)\ \} \quad = \text{set of the inputs}$$

$\mathbb{X}$ and $\mathbb{U}$ are normed linear spaces with norm $\|\cdot\|_p$ of dimension n and m, respectively, where $\underline{x}(k) \in \mathbb{X}$ and $\underline{u}(k) \in \mathbb{U}$. In terms of these sets, the DOC is defined as:

Definition D.1 (DOC): The **degree of controllability**, $DOC(k_N,k_0)$ of a linear discrete-time system of Eq.(2-50) over N steps in the interval $[k_0,k_N]$, is the minimum gain of the linear operator, G, at the initial state, $\underline{x}_o = \underline{x}(k_0)$, which describes the input-state relation of (2-50), that is [28] :

$$DOC(k_N, k_0) = \inf_{G} \left\{ \frac{\| \Delta \underline{x}(k) \|_p}{\| \underline{u}(k) \|_p} \right\} \tag{2-51}$$

where G is the relation between the input space $\mathbb{U}$ and the state space $\mathbb{X}$, namely:

$$G = \{ (\Delta \underline{x}(k), \underline{u}(k)) : \Delta \underline{x}(k) \in \mathbb{X}, \underline{u}(k) \in \mathbb{U}, (\Delta \underline{x}(k), \underline{u}(k)) \neq (0,0) \ \& \ (\infty,\infty) \} \tag{2-52}$$

$\Delta \underline{x}(k) = \underline{x}(k) - \underline{x}^{specified}$ $\underline{x}(k)$ is the solution to Eq.(2-50).

Note that if the norm p=2 then the input space $\mathbb{U}$ is $\|\bullet\|_2$-space and the DOC can be considered as representing the degree of control accomplished when using an energy bounded controller. Moreover, if the system is not controllable then DOC = 0.

To illustrate the mapping G of (2-52), we note that at $k=k_N$, consider the solution of Eq. (2-50) given by:

$$\underline{x}(k) = \Phi(k, k_0)\, \underline{x}_0 + \sum_{i-k_0}^{k-1} \mathbf{F}_c(k-1, i)\, \underline{u}(i) \tag{2-53}$$

where $\mathbf{F}_c(k,i) = \Phi(k,i)\Theta(i)$, and $\Phi(k,i)$ is the transition matrix of the system from the state at time i to the state at k with zero input. This solution can be rewritten as:

$$\underline{x}(k_N) = \mathbf{F}(k,k_0)\, \underline{x}(k_0) + \mathbf{M}_c(k_N,k_0)\, \underline{U}(k_N,k_0) \tag{2-54}$$

where $\mathbf{M}_c(k,k_0)$ is an (n-by-mxk) **controllability matrix** given by:

$$\mathbf{M}_c(k,k_0) = [\Theta(k-1) \mid \Phi(k,k-1)\Theta(k-2) \mid \Phi(k,k-3)\,\Theta(k-3) \mid \cdots \mid \Phi(k,1)\,\Theta(k_0)] \tag{2-55}$$

$\underline{U}(k,k_0)$ is a vector in $\mathbb{R}^{mxk}$ made up of a sequence of input vectors given by:

$$\underline{U}(k,k_0) = [\, \underline{u}^T(k-1) \mid \underline{u}^T(k-2) \mid \underline{u}^T(k-3) \mid \cdots \mid \underline{u}^T(k_0)\,]^T \tag{2-56}$$

Thus the mapping G is the matrix $\mathbf{M}_c(k_N,k_0)$ of (2-55). This mapping is not 1:1, since Eq. (2-54) represents n equations in mxk unknowns, $\underline{U}(k_N,k_0)$. This means that there are many control sequences $\{\underline{u}(0), \underline{u}(1), \underline{u}(2),\ldots,\underline{u}(k-1)\}$ that will return the system states to the origin at k_N. The usual approach to solving Eq(2-54) for $\underline{U}(k_N,k_0)$ is to obtain the mean square solution (i.e, the pseudo inverse of $\mathbf{M}_c(k_N,k_0)$), namely

$$\underline{U}(k_N,k_0) = -\, \mathbf{M}_c^T(k_N,k_0)\, \Phi^T(k_0,k_N)\, [\Phi(k_0,k_N)\, \mathbf{M}_c(k_N,k_0)\, \mathbf{M}_c^T(k_N,k_0)\, \Phi^T(k_0,k_N)\,]^{-1} \underline{x}(k_0)$$

Which can be written using the controllability grammian $\mathbf{W}_c(k_N, k_0)$ as:

$$\underline{U}(k_N,k_0) = -\, \mathbf{M}_c^T(k_N,k_0)\, \Phi^T(k_0,k_N)\, [\mathbf{W}_c(k_N, k_0)\,]^{-1}\ \underline{x}(k_0) \tag{2-57}$$

where $\mathbf{W}_c(k_N,k_0)$ is the (n-by-n) **controllability grammian** matrix given by:

$$\mathbf{W}_c(k_N,k_0) = \mathbf{F}(k_0, k_N)\,[\mathbf{M}_c(k_N,k_0)\,\mathbf{M}_c^T(k_N, k_0)]\,\mathbf{F}^T(k_0, k_N) \qquad (2\text{-}58)$$

or

$$\mathbf{W}_c(k_N, k_0) = \sum_{i=k_0}^{k_{N-1}} \Phi(k_0, i)\,\Theta(i)\,\Theta^T(i)\Phi^T(k_0, i) \qquad (2\text{-}59)$$

Note that if the matrix $\mathbf{W}_c(k_N,k_0)$ is singular then the system is uncontrollable. The only way $\mathbf{W}_c(k_N,k_0)$ can be singular is if the matrix $\mathbf{M}_c(k_N,k_0)$ is not of maximal rank (i.e., rank$\{\mathbf{M}_c(k_N,k_0)\}< n$). This can be shown by observing that each column vector of $\mathbf{M}_c(k_N,k_0)$ represents a vector in the state space along which control is possible. For the system to be controllable in the whole space $\mathbf{R}^n$, it must be controllable in n linearly independent directions in the state space, or in terms of Eq.(2-54), the matrix $\mathbf{M}_c(k_N,k_0)$ must contain n linearly independent column vectors which form a basis in $\mathbf{R}^n$ (that is, the range space of $\mathbf{M}_c(k_N,k_0)$ is equivalent to the state space, $\mathbf{R}^n$).

Next consider the evaluation of the DOC of Def. D1. If the $\underline{x}^{specified}$ is the origin (i.e., $\underline{x}^{specified}=0$) then the $D\underline{x}(k) = \underline{x}(k)$ of Eq.(2-54) and the DOC of Eq.(2-51) can be evaluated using Eq.(2-54). Specifically, if the norm in Eq.(2-51) is p=2, then the N step degree of controllability at k_0 for the linear system of Eq.(2-50) is the square root of the smallest eigenvalue of the controllability grammian $\mathbf{W}_c(k_N, k_0)$ [28], that is:

$$DOC_1(k_N, k_0) = [\,\lambda_{min}\,(\mathbf{W}_c(k_N, k_0))\,]^{1/2} \qquad (2\text{-}60)$$

where $\lambda_{min}(\mathbf{W}_c(k_N, k_0))$ is the smallest eigenvalue of the controllability grammian matrix

Fact F1(Müller and Weber [29]): The degree of controllability of Eq. (2-60) represents the gain G of linear system of Eq.(2-50) under minimum energy , i.e., when $\|\underline{u}(k)\|_2$ = minimum , where

$$\|\underline{u}(k)\|_2 = [\,\sum_{i=1}^{m} |u_i(k)|^2\,]^{1/2}$$

Moreover, the direction in the $\mathbb{X}$-space associated with λ_{min} (dictated by the eigenvector of $\mathbf{W}_c(k_N, k_0)$) is the worst controllable directions of the system of Eq.(2-50), namely the influence of the control action is smallest as compare to the other directions.

Remark: The DOC of Eq.(2-60) and Fact F1 give only part of the information provided

by the controllability grammian , $\mathbf{W}_c(k_N, k_0)$, about the controllability of system of Eq.(2-50). For example, if $\mathbf{W}_c(k_N, k_0)$ is orthogonal, then according to Fact F1 all direction in X-space are "worst controllable", so that one needs other measures which give structural information about the mapping G in addition to the DOC of (2-60).

A viable candidate which gives additional structural information about the mapping G is the condition number of $\mathbf{W}_c(k_N, k_0)$ [30]. This measure gives another DOC:

Definition D2 (DOC based on Condition Number of $\mathbf{W}_c(k_N, k_0)$ [30]):

The degree of controllability of a deterministic linear discrete-time system, Eq.(2-50), is given by the inverse of the condition number of the controllability grammian matrix:

$$DOC_2(k_N,k_0) = \frac{1}{\text{cond}(\mathbf{W}_{cN}(k_N,k_0))} = \frac{\| \mathbf{W}_{cN}^{-1}(k_N,k_0) \|_2}{\| \mathbf{W}_{cN}(k_N,k_0) \|_2} \qquad (2\text{-}61)$$

where cond(**A**) is the condition number of matrix **A**

$$\text{cond}(\mathbf{A}) = \frac{\|\mathbf{A}\|_2}{\|\mathbf{A}^{-1}\|_2} \qquad (2\text{-}62)$$

(Note that $\| A \|_2$ is the largest eigenvalue, λ_{max} , of A and $\| A^{-1} \|_2$ is the smallest eigenvalue, λ_{min}, of A.)

Fact F2: $DOC_2(k_N,k_0)$ takes on values in $0 \le DOC_2 \le 1$, where $DOC_2 = 0$ implies that the system is uncontrollable while $DOC_2 = 1$ implies that all direction in the $\mathbb{X}$-space are equally controllable in terms of requiring the same control energy (since the controllability grammian $\mathbf{W}_c(k_N,k_0)$ matrix is orthogonal).

Additional structural information about the mapping G can be obtained by considering the **Recovery Region**, $\mathbb{R}(k_N, k_0)$ [31-36], which is the set all the initial states, $\underline{x}(k_0)$, that can be returned to the zero state in N steps by any bounded control, that is:

Definition D3 (Recovery Region in terms of finite-time bounded-control):

The N-step **Recovery Region**, $\mathbb{R}(N)$ at k_0 of a discrete-time system is defined as the set of initial states, $\underline{x}_0$, that can be returned to the origin in N steps in the interval $[k_0, k_N]$ with a bounded control:

$$\mathbb{R}(N) = \{\underline{x}_0 := \underline{x}(k_0), \in \mathbf{R}^n \mid \text{there exists a } \underline{u}(k) \in \mathbb{U},\ k \in [k_0, k_N],\ \text{such that } \underline{x}(k_N)=0 \text{ in } N \text{ steps}\}$$

$$\text{where } \mathbb{U} := \{\ \underline{u}(k) \in \mathbf{R}^m\ ,\ |u_i(k)| \le 1 \text{ for } i=1,2,...,m\ \}. \qquad (2\text{-}63)$$

For the linear discrete-time system of Eq.(2-50), the recovery region, $\mathbb{R}(N)$, can be defined as (using the solution of Eq.(2-54), when $\underline{x}(k_N)=0$):

$$\mathbb{R}(N) = \{\underline{x}_0 \in \mathbf{R}^n \mid \underline{x}_0 = -[\Phi(k,k_0)]^{-1}\, \mathbf{M}_c(k_N,k_0)\, U(k_N,k_0),\quad |u_i(k)| \le 1\ \forall\ i\} \qquad (2\text{-}64)$$

This $\mathbb{R}(N)$ is a polytope in the n-dimensional $\mathbb{X}$-space as shown in Figure A-1 for a 2nd order system. Note that the equation describing the $\mathbb{R}(N)$-region is characterized by many constraints and only the binding ones are the relevant ones.

Since in general, it is impractical to monitor the DOC using the $\mathbb{R}(N)$-region characterization given in Eq.(2-64), we shall, instead, characterize it in terms "size", "shape" and "location", specifically:

- The "size" is indicated by the volume of $\mathbb{R}(N)$-region, $\text{Vol}\{\mathbb{R}(N)\}$.
- The "location" is indicated by the "center" of the $\mathbb{R}(N)$-region, denoted by $\underline{x}_0^c$.
- The "shape" is indicated by the positive definite matrix Q which defines the largest imbedded ellipsoid.

All the above structural information about the $\mathbb{R}(N)$-region can be obtained by solving the following optimization problem:

Problem P.1 (Approximation of the Recovery Region, $\mathbb{R}(N)$):

Given the recovery region, $\mathbb{R}(N)$, of Eq-(2-64), find the largest approximating hyper-ellipse, E, contained in $\mathbb{R}(N)$, that is:

$$DOC_3(N) = \underset{E \subseteq \mathbb{R}}{\text{Max}} \{\ \text{VOL}(E)\} \qquad (2\text{-}65)$$

where

$$E = \left\{\underline{x}(0) : \| [C](\underline{x}_0 - \underline{x}^c)\|_2 \le r\right\} \qquad (2\text{-}66)$$

$$\text{VOL}(E) = \frac{\beta\, r^2}{|C|} \qquad (2\text{-}67)$$

$$\beta = \frac{\pi^{n/2}}{\Gamma\left(\frac{n+2}{2}\right)} \qquad (2\text{-}68)$$

R i s the recovery region, $\mathbb{R}(N)$

C is an upper triangular matrix, whose diagonal elements $c_{ii} > 0$, for all i

$\underline{x}^c$ is the center of the recovery region

r is the radius of the hyperellipse

$\Gamma(.)$ is the gamma function

Remark: (i). The DOC_3 of Eq.(2-65) represents the approximate"size" of $\mathbb{R}(N)$.

(ii) The vector $\underline{x}^c$ is the center of $\mathbb{R}(N)$.

(iii) The matrix C gives the shape of $\mathbb{R}(N)$, since $Q = C^TC$ is the positive definite matrix defining the hyperellipse $\mathbb{E}$.

An illustration of the solution of Problem P.1 is shown in Figure A.3 which show the largest hyperellipse embedded in the $\mathbb{R}(N)$-region for a 2nd order system.

Fact F3: The radius r of the hyperellipse $\mathbb{E}$of Eq. (2-66) gives an approximate value of the gain G of linear system of Eq.(2-50). Moreover, the eigenvectors associated with λ_{min} of C-matrix gives the worst controllable directions of the system of Eq.(2-50), namely the direction in which the influence the control action is smallest as compare to the other directions.

A set of software was developed to solve the optimization problem of Problem P1. It is described in Appendix A. This software investigates the robustness of linear time invariant system, and determines the degree of controllability of the system under uncertainty d. The function of the software is:

1. To solve the optimization problem Problem P1.
2. To graphically display the $\mathbb{R}(N)$-region in $\mathbb{X}$-space of the LTI system.
3. To graphically display the regions of δ-space of the LTI system.
4. To display the approximating hyperellipse to the $\mathbb{R}(N)$-region in the $\mathbb{X}$-space.
5. To display the approximate regions in the δ-space which are based on a prescribed degree of controllability (DOC).

Figure 2.10 gives a structured diagram of this software and shows some of the specific capabilities of the software. There are two main options of the controllability robustness software One, investigates the recovery region while the other investigates the allowable uncertainty region in the d-parameter space. Referring to Fig. 2.10, the branch denoted by **SYSDAT** is the data file containing all the information about the LTIS and the parameter

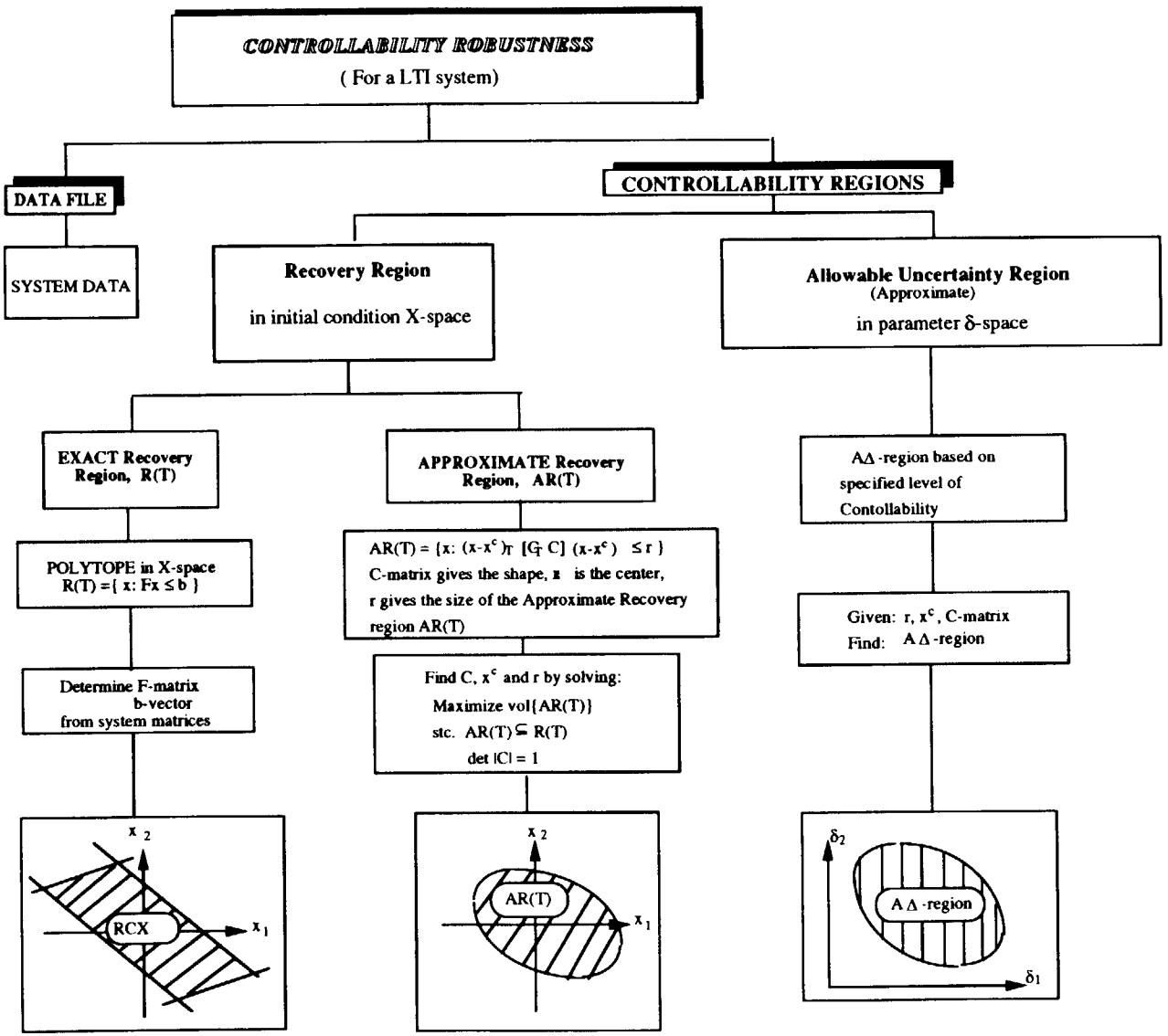

Fig.2.20 Software structure for studying the controllability robustness of LTI systems

uncertainty. The branch whose heading is the **Exact Recovery Region** obtains the $\mathbb{R}(T=N\Delta t)$-region of Definition D3, where $T=N\Delta t$ is the total time of the application of the control. Specifically, the software computes the set of linear inequalities $\{ Fx \leq b \}$ and determines the binding constraints which define $\mathbb{R}(N\Delta t)$. This is illustrated in Fig. 2.11, which shows the region $\mathbb{R}(N\Delta t)$ when $T = N\Delta t = 0.3$ sec. for a 2nd order linear system given by:

$$G(s) = \frac{1}{s^2 + 3s + 2}$$

or

$$\dot{x} = \begin{bmatrix} 0 & 1 \\ -2 & -3 \end{bmatrix} \begin{bmatrix} x_1 \\ x_2 \end{bmatrix} + \begin{bmatrix} 0 \\ 1 \end{bmatrix} u$$

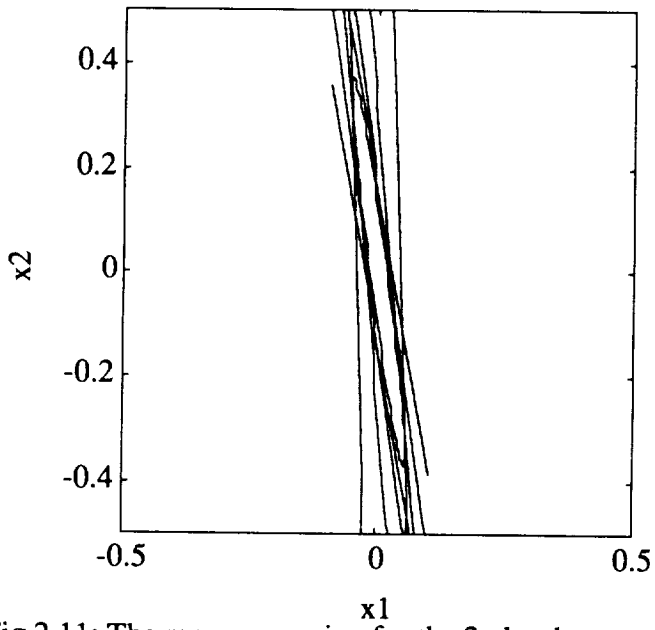

Fig.2.11: The recovery region for the 2nd order system, T=0.3

The discrete time system representation using Eq.(A-3) of the appendix when $\Delta t = 0.075$ sec and $n= 15$, is the system model of Eq.(2-50) when

$$\Phi = \begin{bmatrix} 0.995 & .067 \\ -.134 & .794 \end{bmatrix}; \qquad \Theta = \begin{bmatrix} .0026 \\ .067 \end{bmatrix}$$

Referring to Fig. 2.10, the branch whose heading is the **Approximate Recovery Region**, AR(T), finds the best approximation of the $\mathbb{R}(T=N\Delta t)$-region given by the hyperellipse $\mathbb{E}$ of Eq. (2-66). Specifically, it solves Problem P1 to obtain the shape (matrix C), the location (center x^c) and the size (radius, r) of the $\mathbb{R}(T=N\Delta t)$-region. Figure 2.12 illustrates the $\mathbb{AR}(T=N\Delta t)$-region for the $\mathbb{R}(T=N\Delta t)$-region shown in Fig. 2.11. The

radius r = 0.079 and the matrix C is

$$C = \begin{bmatrix} 4.697 & .6834 \\ 0 & .2129 \end{bmatrix}$$

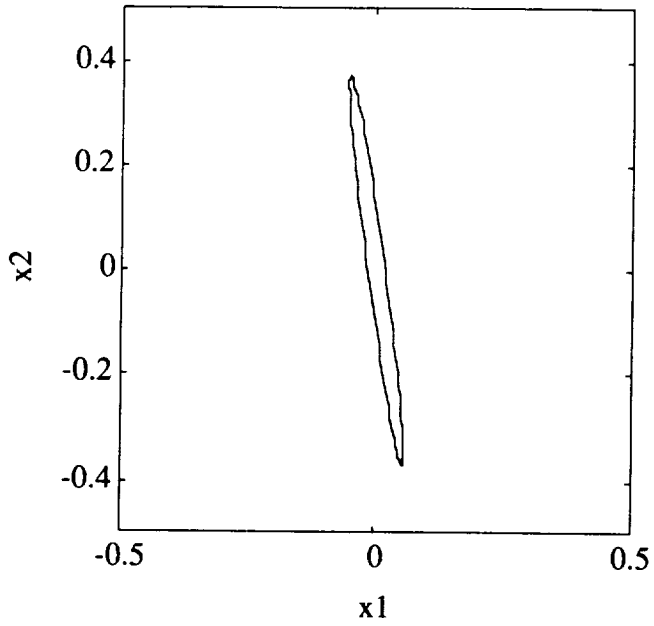

Fig.2.12: The approximatie recovery region for the 2nd order system when the control period T=0.3

Referring to Fig. 2.10, the branch whose heading is the **Allowable Uncertainty region** $A\Delta(T)$, finds the set of values of the uncertainty parameters in the δ-space. Specifically,

$$\mathbb{A}\Delta(T=N\Delta t) = \{\delta : G(s;\delta) \text{ gives a level of controllability as prescribed by a } \mathbb{R}(T=N\Delta t)\text{-region}\} \quad (2\text{-}69)$$

where $G(s;\delta)$ is the transfer function of the LTI system. This $\mathbb{A}\Delta(N\Delta t)$ can be defined in terms of the structural indicators of $\mathbb{R}(N\Delta t)$ given by the C-matrix, center x^c and radius r as follows:

$$\mathbb{A}\Delta(N\Delta t) = \{\delta : G(s;\delta) \text{ gives a level of controllability specified by triplet } (C,x^c,r)\} \quad (2\text{-}70)$$

At present, this part of the software has not yet been developed. What has been implemented are the two branches shown in Fig. 2.10 under the heading **Recovery Region**. Based on preliminary tests, the software works well except when the hyperellipse is ill-conditioned (i.e., when the C-matrix is ill-conditioned). We suspect that

this is due to our choices of the termination conditions in the (C,r) optimization algorithm of Fig. A.3 and the overall optimization method of Fig. A.4 given in Appendix A.

To initiate the design of the software indicated by branch in Fig. 2.10 whose heading is the **Allowable Uncertainty region,** $A\Delta(T)$, we performed sensitivity studies to determine the type of variation to be expected in $\mathbb{R}$-region when the system parameters change. Specifically, for the system

$$G(s) = \frac{1}{s^2 + as + b}$$

we studied the effect of variation of the coefficients a and b on the triplet (C,x^c,r). Figure 2.13 shows the $\mathbb{R}$-region when a = b = 1.414. Note that this $\mathbb{R}$-region changed both in size and orientation from that shown in Fig. 2.11. This changed is measured by a different values of r = .0464 and C-matrix

$$C = \begin{bmatrix} 4.76 & 0.8 \\ 0 & .21 \end{bmatrix}$$

The center $x^c = 0$, the origin of the $\mathbb{X}$-space. This is the usual case because of the definition of the $\mathbb{R}$-region.

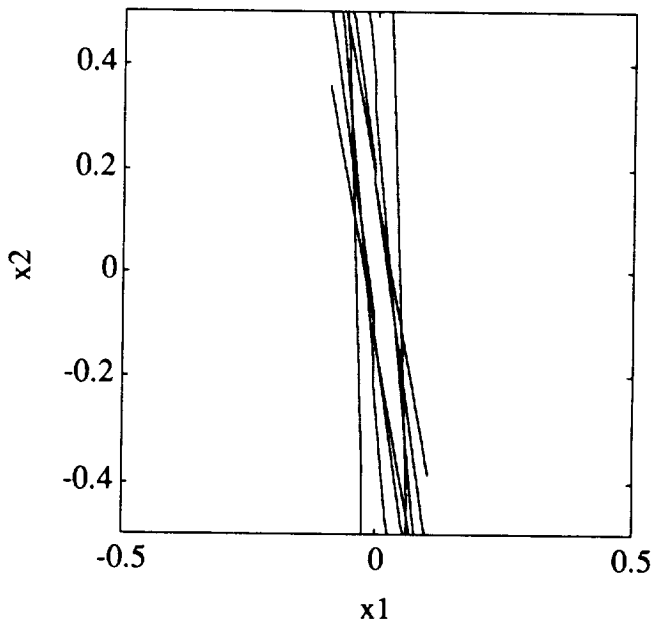

Fig.2.13: Recovery region for a 2nd order system, T=0.3

3. SUMMARY OF THE WORK

Task 1: Design of Robust Optimal Controllers via H^∞ Approach

Task 1.1: Study of the aircraft flight guidance/control models and problems provided by the Aircraft Guidance and Control Branch, NASA Langley Research Center.

Status: In the process of obtaining appropriate practical aircraft flight guidance/control models from AGCB scientists. Before the models arrive, we use a hypothetical model with plant perturbations and uncertain disturbances.

Accomplishment: A procedure to represent plant perturbations and uncertain disturbances as H^∞ models is presented.

Task 1.2: Formulation of the aircraft flight guidance/control problems as a robust H^∞ optimization problem with unstructured and parametric uncertainties.

Status: Before the practical models arrive, a hypothetical model is used to demonstrate how to formulate a robust H^∞ optimization problem.

Accomplishment: A detailed procedure to formulate a robust H^∞ optimization problem is presented. See [Pub 1,2] for details.

Task 1.3: Computation of the H^∞ norm of a given transfer function.

Status: 100% of the proposed work has been done. See [Pub 3] for details.

Accomplishment: The pole-zero diagram of G(s), the root locus concept, and the $j\omega$-axis transmission zeros of $\gamma^2 I - G^T(-s)G(s)$ are employed to quickly locate a narrow frequency interval which brackets the supremum of $\bar{\sigma}[G(j\omega)]$. Then Brent's method (an improved parabolic interpolation search method) is employed to search for the supremum of $\bar{\sigma}[G(j\omega)]$ over the frequency interval.

Task 1.4: Solution of the robust H^∞ optimization problem.

Status: 100% of the proposed work has been done. See [Pub 4,5,6] for details.

Accomplishment: Some useful properties of the two H^∞ Riccati solutions have been discovered. Among them, the most prominent one is that the spectral radius of the product of these two Riccati solutions is a continuous, nonincreasing, convex function of γ in the domain of interest. Based on these properties, quadratically convergent algorithms are developed to compute the optimal H^∞ norm.

Task 1.5: Algorithm development for the computational problems arising in the

robust H^∞ optimization problem.

Status: 60% of the proposed work has been done. See [Pub 4-8] for details.

Accomplishment: The algorithm to compute the optimal H^∞ norm and the construction of an optimal or a suboptimal H^∞ controller are presented.

Task 1.6: Computer simulation.

Status: 40% the proposed work has been done.

Accomplishment: The time-domain and frequency-domain behavior of the closed-loop system for the hypothetical model has been tested.

Task 2: Design of Robust Optimal Controllers via Mixed H^2/H^∞ Approach

Task 2.1: Formulation of the aircraft flight guidance/control problems provided by the Aircraft Guidance and Control Branch, NASA Langley Research Center as a mixed H^2/H^∞ optimization problem with unstructured uncertainties.

Status: In the process of obtaining appropriate practical aircraft flight guidance/control models from AGCB scientists. Before the practical models arrive, a hypothetical model is used to demonstrate how to formulate an H^∞/H^2 optimization problem.

Accomplishment: A procedure to formulate an H^∞/H^2 optimization problem is presented. See [Pub 9-12] for details.

Task 2.2: Solution of the mixed H^2/H^∞ optimization problem.

Status: An important special case of the mixed H^2/H^∞ optimization problem has been completely solved.

Accomplishment: In case that the H^2 and the H^∞ transfer functions are identical, the mixed H^2/H^∞ problem can be solved by H^∞ technique with γ a free parameter. Then γ is used to trade off H^∞ robustness against H^2 performance. See [Pub 9-12] for details.

Task 2.3: Plotting the H^2/H^∞ curve and using it for robust controller design.

Status: 80% of this study has been done.

Accomplishment: A graphical method to determine the best γ for H^∞ robustness and H^2 performance is proposed. See [Pub 11,12] for details.

Task 2.4: Algorithm development for the computational problems arising in the he mixed H^2/H^∞ optimization problem.

Status: 40% of the proposed work has been done. See [Pub 11,12] for details.

Accomplishment: Algorithms to generate the H^2/H^∞ curve and the construction of an H^2/H^∞ controller are presented.

Task 2.5: Computer simulation.

Status: 40% the proposed work has been done.

Accomplishment: The time-domain and frequency-domain behavior of the closed-loop system for the hypothetical model has been tested.

Task 3: Construction M-Δ Structure

Task 3.1: Construction of an M-Δ structure of a system with parametric uncertainties for robust stability analysis.

Status: 100% of the proposed work has been done. See [Pub 16-17] for details.

Accomplishment: A systematic way of constructing an M-Δ structure of a system with parametric uncertainties for robust stability analysis is presented.

Task 3.2: Construction of an M-Δ structure of a system with parametric and unmodelled uncertainties for robust stability analysis.

Status: 100% of the proposed work has been done. See [Pub 16-17] for details.

Accomplishment: A systematic way of constructing an M-Δ structure of a system with parametric and unmodelled uncertainties for robust stability analysis is presented.

Task 3.3: Construction of an M-Δ structure of a system with parametric and unmodelled uncertainties for robust stability and robust performance analysis.

Status: 100% of the proposed work has been done. See [Pub 16-17] for details.

Accomplishment: A systematic way of constructing an M-Δ structure of a system with parametric and unmodelled uncertainties for robust stability and robust performance analysis is presented.

Task 3.4: Verification of the minimality of an M-Δ structure of a system.

Status: 30% of the proposed work has been done. See [Pub 16-17] for details.

Accomplishment: We show that if the dimension of Δ is the least number of assigned parameters such that the coefficients of the corresponding characteristic polynomial are multilinear functions of the assigned parameters, then the M-Δ structure is minimal.

Task 3.5: Construction of a minimal M-Δ structure.

Status: 30% of the proposed work has been done. See [Pub 16-17] for details.

Accomplishment: For the case that the state-space realization is a linear function of the uncertainties, a minimal M-Δ structure can be constructed in a systematic way.

Task 4: Controllability and Observability of Perturbed Plant

Task 4.1: Controllability.

Status: 70% of the proposed work has been done.

Accomplishment: Developed (i) a software package for investigating the controllability robustness of linear time invariant systems. This software obtains the size, shape and location of the recovery region, and (ii) relation between the various DOC measures encountered in the literature.

Task 4.2 Observability

Status: No work performed.

Task 4.3 Integration of Controllability and Observability Concepts into the Overall Robust Controller design

Status: No work has been performed as yet.

Publications:

[Pub 1] B. C. Chang, X. P. Li, S. S. Banda, and H. H. Yeh, "Robust Control Systems Design by H∞ Optimization Theory," Proceedings of the 1991 AIAA Guidance, Navigation, and Control Conference, Aug. 1991.

[Pub 2] X. P. Li, B. C. Chang, S. S. Banda, and H. H. Yeh, "Robust Control Systems Design by H∞ Optimization Theory," To appear in AIAA Journal of Guidance, Control, and Dynamics.

[Pub 3] B. C. Chang, X. P. Li, S. S. Banda and H. H. Yeh, "Computation of the H∞ Norm of a Transfer Function," Proceedings of the 1990 American Control conference, pp. 2578-2582, San Diego, May, 1990.

[Pub 4] X.P. Li and B.C. Chang, "On Convexity of H∞ Riccati Solutions and Its Applications," To appear in IEEE Transactions on Automatic Control.

[Pub 5] X.P. Li and B.C. Chang, "On Convexity of H∞ Riccati Solutions," To appear in the Proceedings of IEEE Conference on Decision and Control, Dec. 1991.

[Pub 6] X.P. Li and B.C. Chang, "Properties of H∞ Riccati Equations," Proceedings of the 1991 International Workshop on Robust Control, Sponsored by NSF, AFOSR, and Texas A & M, San Antonio, March, 1991.

[Pub 7] B. C. Chang, X. P. Li, H. H. Yeh, and S. S. Banda, "Iterative Computation of the Optimal H∞ Norm By Using Two-Riccati-Equation Method," Proceedings of IEEE Conference on Decision and Control, Dec. 1990.

[Pub 8] B. C. Chang, X. P. Li, S. S. Banda, and H. H. Yeh, "Design of an H∞ Optimal Controller By Using DGKF's State-space Formulas", Proceedings of IEEE Conference on Decision and Control, Dec. 1990.

[Pub 9] H. H. Yeh, S. S. Banda, and B. C. Chang, "Necessary and Sufficient

Conditions for Mixed H^2 and H^∞ Optimal Control," To appear in IEEE Transactions on Automatic Control.

[Pub 10] H. H. Yeh, S. S. Banda, and B. C. Chang, "Necessary and Sufficient Conditions for Mixed H2 and H∞ Optimal Control", Proceedings of IEEE Conference on Decision and Control, Dec. 1990.

[Pub 11] C. C. Belcastro, B. C. Chang, R. Zong, and R. Fischl, "Design of a Suboptimal H^∞ Controller with H^2 and Bandwidth Constraints", Proceedings of the 1991 American Control Conference, June 1991.

[Pub 12] H. Bouguerra, B.C. Chang, H.H. Yeh, and S.S. Banda, "A Robust H∞ Controller Design with H2 Consideration," To appear in the Proceedings of IEEE Conference on Decision and Control, Dec. 1991.

[Pub 13] H. Bouguerra, B. C. Chang, H. H. Yeh, and S. S. Banda, "Fast Stability Checking for the Convex Combination of Stable Polynomials," IEEE Transactions on Automatic Control, Vol. 35, No. 5, pp. 586-588, May 1990.

[Pub 14] B. C. Chang, O. Ekdal, H. H. Yeh, and S. S. Banda, "Computation of the Real Structured Singular Value via Polytopic Polynomials," AIAA Journal of Guidance, Control, and Dynamics, Vol. 14, No. 1, pp. 140-147, Jan. 1991.

[Pub 15] O. Ekdal and B. C. Chang, "Robust Stability Analysis of Real Structured Uncertain Systems", Proceedings of the 11th IFAC (International Federation of Automatic Control) World Congress, Aug. 1990, Tallinn, USSR.

[Pub 16] C. C. Belcastro, B. C. Chang, and R. Fischl, "A Methodology for Formulating a Minimal Uncertainty Model for Robust Control System Design and Analysis", Proceedings of the 3rd Annual Conference on Aerospace Computational Control, pp.355-369, December, 1989.

[Pub 17] C. C. Belcastro, B. C. Chang, and R. Fischl, "On the Formulation of a Minimal Uncertainty Model for Robust Control with Structured Uncertainty," NASA Technical Paper 3094, Sept. 1991.

4. CONCLUSION AND WORK FOR FUTURE RESEARCH

4.1 Conclusion

In [Pub 4] we revealed several important eigen properties of the stabilizing solutions of the two H^∞ Riccati equations and their product. Among them, the most prominent ones are: (1) $\rho[X_\infty(\gamma)Y_\infty(\gamma)]$ is a nonincreasing, convex function of γ on $(\beta,+\infty)$. (2) $\lambda_{min}[\hat{X}(\gamma)]$ is a nondecreasing, concave function of γ on $(\alpha_x,+\infty)$. (3) $\hat{X}(\gamma)$ is invertible almost everywhere on $(\alpha_x,+\infty)$. Based on these properties, quadratically convergent algorithms [Pub 5,6] were developed to compute the γ_∞, the optimal H^∞ norm, such that $\rho[X_\infty(\gamma_\infty)Y_\infty(\gamma_\infty)] = \gamma_\infty^2$ and to compute β, the infimum of γ such that the two H^∞ Riccati equations have positive semidefinite stabilizing solutions.

The formulation of the standard H^∞ optimization problem, an easy way of constructing a state-space realization of the generalized plant, an efficient algorithm for computing the optimal H^∞ norm, and a modified version of Glover and Doyle formulas for constructing an optimal controller were addressed in the paper [Pub 2]. No numerical

difficulty will arise in constructing an H^∞ optimal controller if we are allowed a proper controller. In most applications, we may like to have a strictly proper controller with limited bandwidth. In this case, a trade-off between the H^∞ performance and the bandwidth should be made by degrading the H^∞ norm from its optimum in order to reduce the controller bandwidth.

In [Pub 11], we found an easy way to trade off the H^∞ robustness and H^2 performance for the case that H^∞ and H^2 transfer functions are the same. In general, these two transfer functions may be different. In [Pub 12], we formulated a more realistic control problem with H^2 performance index and H^∞ stability robustness constraint into a mixed H^2/H^∞ problem. No optimal solution yet is available for this more general mixed H^2/H^∞ problem. Although the optimal solution for this mixed H^2/H^∞ control has not yet been found, we proposed a design approach which can be used through proper choice of the available design parameters to influence both robustness and performance.

The theoretical work in controllability on developing a relation between the various degree of controllability (DOC) measures encountered in the literature, indicates that there is a relation and what is needed now to establish the specific relations. The simulation work concentrated on developing software for investigating the controllability robustness of linear time invariant systems. A preliminary software package (described in Appendix A) was developed for measuring the size, shape and location of the recovery region. Initial indications show that the various optimization algorithms (needed to automatically obtain the value of the indicators) work, however they may need some refinements in order to take care of such problems as obtaining DOCs for ill-conditioned recovery regions.

4.2 Work for Further Research

4.2.1 M-Δ Structure and Robust Stability Analysis for Structured Uncertainties

M-Δ structure is a rearrangement of a perturbed system where M(s) is the nominal system and Δ is a block diagonal matrix which consists of all the perturbations. M-Δ structure is essential in the SSV(structured singular value) analysis and design techniques. Although Δ is assumed stable, the M-Δ structure can handle a large class of uncertainties which include unstable perturbation, i.e., the number of unstable poles of the perturbed plant can be different from that of the nominal plant. It is always possible to pull out all uncertain parts from a perturbed system and form an M-Δ structure. However, very little about how to obtain this structure has been addressed in the literature. A systematic

procedure for constructing M-Δ structure is proposed.

A minimal M-Δ structure means that the dimension of Δ (or M) of the M-Δ structure is minimal. We can construct an M-Δ structure for a given perturbed system, but the dimension of the structure may be unnecessarily large. A nonminimal structure will cause unnecessary complexity in computation and therefore a minimal M-Δ structure is essential in the computation of the SSV. So far, only some special cases of the minimal M-Δ structure problems have been addressed [37,38]. A progress in the construction of a minimal M-Δ structure will greatly simplify robust stability analysis for structured uncertainties.

4.2.2 Design of Robust Flight Control Systems via H^∞ Optimization

In this research period, we developed a fast algorithm to compute the optimal H^∞ norm and to construct an optimal H^∞ controller without numerical difficulty. Next, we will apply this design tool to flight control systems. We will use the H^∞ norm of the complementary sensitivity function as a measure of robust stability and will formulate an H^∞ optimization problem which minimizes the maximum error energy subject to a robust stability constraint. The error reduction and the robust stability can be traded off by choosing the weighting matrices in the cost function. Initially, a weighting matrix is chosen and the corresponding H^∞ optimization problem is solved to obtain an optimal controller. The weighting matrices are modified iteratively until the robust stability constraint is just satisfied. The way the weighting matrices affect the trade-off is only partially understood. In addition to the magnitude of the weighting matrix, the structure of the weighting matrix is also an important factor in the trade-off. We will investigate how the weighting matrices affect the trade-off. We will also develop an iterative updating procedure for the weighting matrices by which a robust controller can be designed such that the closed-loop system is robustly stable and the maximum of error energy is minimized.

4.2.3 Design of Robust Controllers via Mixed H^2/H^∞ Optimization

The optimal H^∞ controller which minimizes the H^∞ optimization problem usually has wide bandwidth and leads to a poor H^2 performance. In [13], we found that a little bit sacrifice of the H^∞ norm will greatly reduce the bandwidth of the controller and improve the H^2 performance tremendously. It is practical to formulate a robust control problem as a that of minimizing an H^2 cost function subject to an H^∞ bound. The H^2 cost function is equivalent to the well known LQG cost function and the H^∞ bound can take care of robust stability and robust error reduction.

In [39], we formulated a more realistic control problem with H^2 performance index and H^∞ stability robustness constraint into a mixed H^2/H^∞ problem. The H^2 and H^∞ transfer functions are different. No optimal solution yet is available for this more general mixed H^2/H^∞ problem. A research in finding an efficient approach for the mixed H^2/H^∞ optimization problem is proposed.

4.2.4 Controllability and Observability of Perturbed Plant

For task 4 in the next research period we will concentrate on: (i) Theoretical work on developing a relation between the various DOC measures encountered in the literature, and determine which of these is most suitable for characterizing the **Allowable Uncertainty region,** $A\Delta(T)$, discussed in Section 2.6. (ii) Improving the algorithms used in developing the Recover Region software shown in Fig. 2.10 Specifically, we will take care of the ill-conditioning problem currently encountered when the recovery region is very narrow. We will also design and develop the **Allowable Uncertainty region,** $A\Delta(T)$, software indicated in Fig. 2.10. (iii) Perform robustness studies for a variation in the system parameters $\{c_i\}$ and $\{b_j\}$ of the system function

$$G(s) = \frac{\Sigma\, b_j s^j}{\Sigma\, c_i s^i}$$

REFERENCES

[1] J. Doyle, K. Glover, P. Khargonekar, and B. Francis, "State-space solutions to standard H_∞ and H_2 control problems," *IEEE Trans. Automat. Contr.*, Vol. AC-34, pp. 831-847, 1989.

[2] K. Glover and J. Doyle, "State-space formulae for all stabilizing controllers that satisfy an H_∞ norm bound and relations to risk sensitivity," *Syst. Contr. Lett.*, Vol. 11, pp. 167-172, 1988.

[3] Carsten Scherer, "H_∞-control by state-feedback and fast algorithms for the computation of optimal H_∞-norms," *IEEE Trans. Automat. Contr.*, Vol. AC-35, pp. 1090-1099, 1990.

[4] P. Pandey, C. Kenny, A. Laub, and A. Packard, "Algorithms for computing the optimal H_∞-norm," Proceedings of the 29th Conference on Decision and Control, Dec. 1990.

[5] B. C. Chang, X. P. Li, S. S. Banda, and H. H. Yeh, "Iterative computation of the optimal H_∞ norm by two-Riccati-eqution method," Proceedings of the 29th Conference on Decision and Control, Dec. 1990.

[6] J. Doyle, "Analysis of Feedback Systems with Structured Uncertainties," *IEE Proceedings*, Vol. 129 Pt.D, No.6, 1982, pp. 242-250.

[7] J. Doyle, "Structured Uncertainty in Control System Design," *Proceedings of the 24th Conference on Decision and Control*, Dec. 1985.

[8] J. C. Doyle and G. Stein, "Robustness with observers," IEEE Trans. Aut. Cont., vol. AC-24, pp. 607-611, Apr. 1979.

[9] G. Stein and M. Athans, ' The LQG/LTR procedure for multivariable feedback control design, ' IEEE Trans. Aut. Contr., Vol. AC-32, pp. 427-429, 1987.

[10] G. Zames, "Feedback and Optimal sensitivity: Model reference transformations, multiplicative seminorms, and approximate inverses, " IEEE Trans. Aut. Contr., vol. AC-26. pp 301-320, 1981.

[11] D. S. Bernstein and W. M. Haddad, " LQG Control with H^∞ Performance Bound," IEEE Trans. Aut. Cont., vol. AC-34, no. 3, March 1989.

[12] K. Zhou, J.C. Doyle, K. Glover and B. Bodenheimer, "Mixed H^2 and H^∞ Control, " Proc. of the 1990 American Control Conference, San Diego, CA pp. 2502-2507.

[13] M. Belcastro, B-C Chang, R. Zong and R. Fischl, " H^∞ control with bandwidth and H^2 constraints, " 1991 American Control Conference.

[14] D. Mustafa, "Relations between maximum-entropy/ H^∞ control and combined H^∞/LQG control, " Systems & Control Letters 12 (1989), pp. 193-203.

[15] R.E. De Gaston and M.G. Safonov, "Exact Calculation of the Multiloop Stability Margin", IEEE Trans. A-C. AC-33, pp. 156-171, 1988.

[16] R.S.S. Pena and A. Sideris, "A General Program to Compute the Multivariable Stability Margin for Systems with Parametric Uncertainty", Proceedings of the 1988 American Control Conference.

[17] V. L. Kharitonov, "Asymptotic Stability of an Equilibrium Position of a Family of Systems of Linear Differential Equations", Differential'nye Uraveniya, Vol. 14, No. 11, pp. 1483-1485, 1978.

[18] A.C. Bartlett, C.V. Hollot, and H. Lin, "Root Locations on an Entire Polytope of Polynomials: It Suffices to Check the Edges", Proceedings of the 1987 American Control Conference.

[19] M. Fu and B.R. Barmish, "Stability of Convex and Linear Combinations of Polynomials and Matrices Arising in Robustness Problems", Proceedings of the Conference on Information Sciences and Systems, John Hopkins University, 1987.

[20] S. Bialas, "A Necessary and Sufficient Condition for the Stability of Convex Combinations of Stable Polynomials or Matrices", Bulletin of the Polish Academy of Sciences, Technical Sciences, Vol. 33, No. 9-10, pp.473-480, 1985.

[21] K.H. Wei and Yedavalli, "Invariance of Strict Hurwitz Property for Uncertain Polynomials with Dependent Coefficients", IEEE Trans. A-C, AC-32, pp. 907-909, 1987.

[22] L.H. Keel, S.P. Bhattacharyya, and J.W. Howze, "Robust Control with Structured Perturbations", IEEE Trans. A-C, AC-33, pp. 68-78, 1988.

[23] H. Bouguerra, B-C Chang, H.H. Yeh, and S.S. Banda, "A Fast Algorithm for Checking the Stability of Convex Combinations of Stable Polynomials", Proceedings of the 28th IEEE Conference of Decision and Control, Dec. 1989.

[24] H. Kwakernaak, "Minimax Frequency Domain Performance and Robustness Optimization of Linear Feedback Systems,"*IEEE Transactions on automatic control*, Vol. AC-30, Oct. 1985, pp.994-1004.

[25] K. Glover, D.J.N. Limebeer, J.C. Doyle, E.M. Kasenally, and M.G. Safonov, "A Characterization of All Solutions to the Four Block General Distance Problem," Preprint, 1989.

[26] B. C. Chang, X. P. Li, S. S. Banda, and H. H. Yeh, "Design of an H_∞ optimal controller by using DGKF's state-space formulas," *Proceedings of the 29th Conference on Decision and Control,* Dec. 1990.

[27] I. Postlethwaite, D.-W. Gu, and S. D. O'Young, "Some computational results on size reduction in H_∞ design", *IEEE Trans. Automat. Contr.*, Vol. 33, pp. 177-185, 1988.

[28] Sevaston, G.E. and Longman, R.W.: " Gain measures of controllability and observability," International Journal of Control, Vol. 41, No.4, p.865-893, 1985

[29] Muller, P.C. and Weber, H.I. : "Analysis and optimization of certain qualities of controllability and observability for linear dynamic systems", Automatica, Vol.8, p.237,1979

[30] Ham, F.M."Determination of the Degree of Observability in Linear Control Systems", Ph.D. Diss., Ohio State University, 1980.

[31] Viswanathan, C.N. , Longman, R.W. and Likins, P.W. : "A degree of controllability definition : Fundamental concepts and application of model system," Journal of Guidance, Contr. and Dynamics, Vol. 7, p.222, Mar.-Apr. , 1984

[32] Longman, R.W. and Alfriend, K.T.," Energy Optimal Degree of Controllability and Observability For Regulator and Manual Problems."Proc., of the Sixteenth Annual Conference On Information Sciences and Systems, Princeton, N.J., March, 1982.

[33] Lindburg, R.E. and Longman, R.W.,"Optimization of Actuator Placement Via Degree of Controllability Criteria Including Spillover Consideration," AIAA/AAS Paper 82-1435, San Diego, California, 1982.

[34] Laskin, R.A., Longman, R.W., and Likins, P.W., "Actuator Placement in Modal Systems Using Fuel Optimal Degree of Controllability Concepts." Proc., of The 20th Annual Allerton Conference on Communication, Control and Computing, Monticello, ILL, October, 1982.

[35] Schmitendorf, W.E., "An Exact Expression for Computing the Degree of Controllability." Journal of Guidance, Control and Dynamics, Vol. 7, pp. 502-504, July-August 1984.

[36] Sokolowski, S.J. and Fischl, R. : "An algorithm for computing the degree of controllability of a discrete time, bounded input, regulator problem", Proceedings of the 1986 ACC.

[37] C. C. Belcastro, B. C. Chang, and R. Fischl, "A Methodology for Formulating a Minimal Uncertainty Model for Robust Control System Design and Analysis", Proceedings of the 3rd Annual Conference on Aerospace Computational Control, pp.355-369, December, 1989.

[38] C. C. Belcastro, B. C. Chang, and R. Fischl, "On the Formulation of a Minimal Uncertainty Model for Robust Control with Structured Uncertainty," NASA Technical Paper 3094, Sept. 1991.

[39] H. Bouguerra, B.C. Chang, H.H. Yeh, and S.S. Banda, "A Robust H∞ Controller Design with H2 Consideration," To appear in the Proceedings of IEEE Conference on Decision and Control, Dec. 1991.

Appendix: Controllability Robustness Software

A.1 Purpose

The purpose of the Controllability Robustness (COR) software is to investigate the effectiveness of the various performance indices used for measuring the degree of controllability of linear time invariant system under uncertainty δ. The function of the software is:

1. To graphically display the **Recovery region**, $\mathbb{R}(T)$, in the X-space.
2. To automatically compute the degree of controllability (DOC) indices which are needed to characterize the controllability of the LTI system.
3. To graphically display the **Approximate Recovery Region**, AR(T) in the X-space.
4. To graphically display the set of parameter variations in the δ-space which are guaranteed to give a specified level of system controllability.

The graphical capabilities is illustrated in Fig. 2.10 (of the report) which gives a structured diagram of this software.

A.2 Method

The method used in obtaining the DOC indices of system is summarized in the flowchart of Figure A.1. The inputs to the program are the matrices {A,B} and the parameter variations, d, of the linear time invariant system

$$\dot{x} = A(\delta)x + B(\delta)u \tag{A-1}$$

Remark: It is planned that once a method for the M-Δ decomposition will be available, then the input to the COR program will be the $G(s,\delta)$ system function.

The system of Eq.(A-1) is sampled with a sampling period, Δt, to obtain the linear discrete time model of Eq.(2-50), namely

$$\underline{x}(k+1) = \Phi(\delta)\,\underline{x}(k) + \Theta(\delta)\,\underline{u}(k) \tag{A-2}$$

where the matrices Φ and Θ are obtained using the power series expansion of the transition matrix

$$\Phi = [\, I + A\Delta t + (A\Delta t)^2/2! + \ldots + (A\Delta t)^n/n! \,] \tag{A-3a}$$

$$\Theta = [\, I + A\Delta t + (A\Delta t)^2/2! + \ldots + (A\Delta t)^n/n! \,]\,\Delta t \tag{A-3b}$$

This is done in the subroutine DSCRET shown in Fig. A.1. Referring to Fig. 2.10, the

program which computes the **Recovery Region,** $\mathbb{R}(T=N\Delta t)$, implements the definition of Eq.(2-64) and computes a set of linear inequalities $\{ Fx \leq b \}$ and then identifies those constraints which are the binding constraints of $\mathbb{R}(N\Delta t)$. This is implemented in subroutine CONTRG shown in Fig. A.1.

The **Approximate Recovery Region**, AR(T), software solves the optimization Problem P1 to obtain the shape (matrix C), the location (center x^c) and the size (radius, r) of the $\mathbb{R}(T=N\Delta t)$-region and then uses this to define the largest embedded hyperellipse in the $\mathbb{R}(T=N\Delta t)$-region. The subroutine which executes the solution of Problem P1 is labeled ELLIPSE in Fig. A.1. The approach to solving Problem P1 is based on the realization that when the matrix C is given then Problem P1 is a Linear Problem (LP) problem. This is exploited in our method as summarized in Fig. A.2. The first step is to set up the linear constraints. Then, depending on if we want to obtain a new matrix C or not we solve either an Linear Problem (LP) problem or a Non Linear Problem (NLP), that is:

LP problem finds the optimum center, x^c, and radius, r, for a given matrix C. The LP problem solves a volume maximization problem in which the embedding hyperellipse $\mathbb{E}$ shape is held constant but its size (i.e., volume of Eq.(2-66)) is maximized by increasing the radius, r, and moving it around inside $\mathbb{R}$ (by moving the center, x^c) while satisfying the constraint $\mathbb{E} \subseteq \mathbb{R}$.

NLP problem finds the matrix C and radius r for a given center x^c. It solves the same volume maximization problem of Eq.(2-66), when the center x^c is fixed. The C-matrix and r are optimized by a sequential unconstrained minimization (SUM) method. The method minimizes an objective function γ_k which is a pth norm of a vector representing the slack variable of the inequalities. The details of the updating method is shown in Fig. A.3. The optimum is found by computing the gradient of γ_k with respect to t_{ij}, the components of the inverse of the C matrix ($T=C^{-1}$). (The reason for using T instead of C in the optimization is because the SUM method has better convergent properties.)

The method for optimizing all three sets of parameters, i.e. C-matrix, x^c and r is shown in Figure A.4. Note that it uses both the NL and the NLP algorithms to solve the optimization problem stated in Problem P1. The subroutine implementing the optimization algorithm shown in Fig. A.4 is called ELLIPSE.

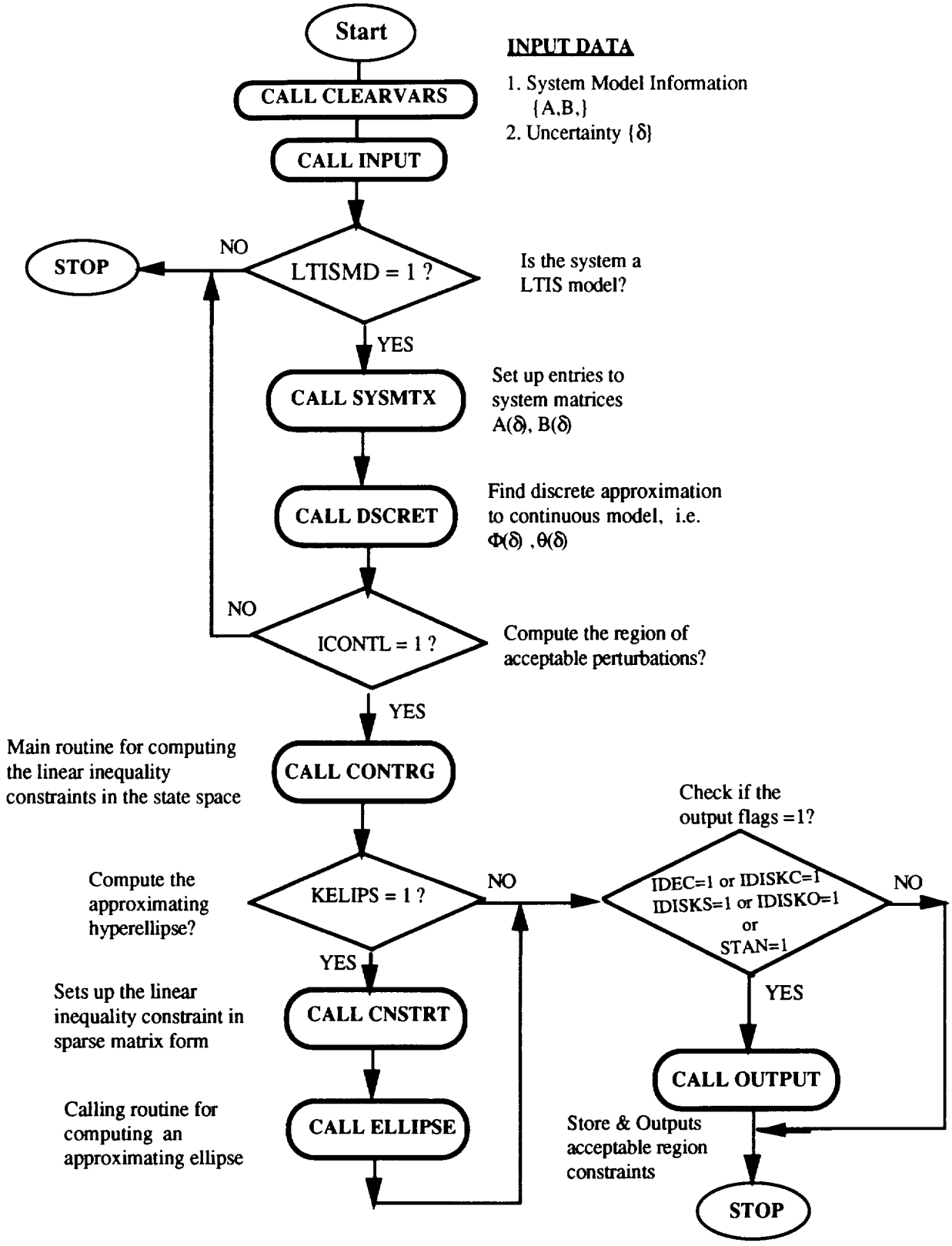

Figure A-1: Flowchart of the COR program for studying the Controllability Robustness of Linear Time Invariant Systems

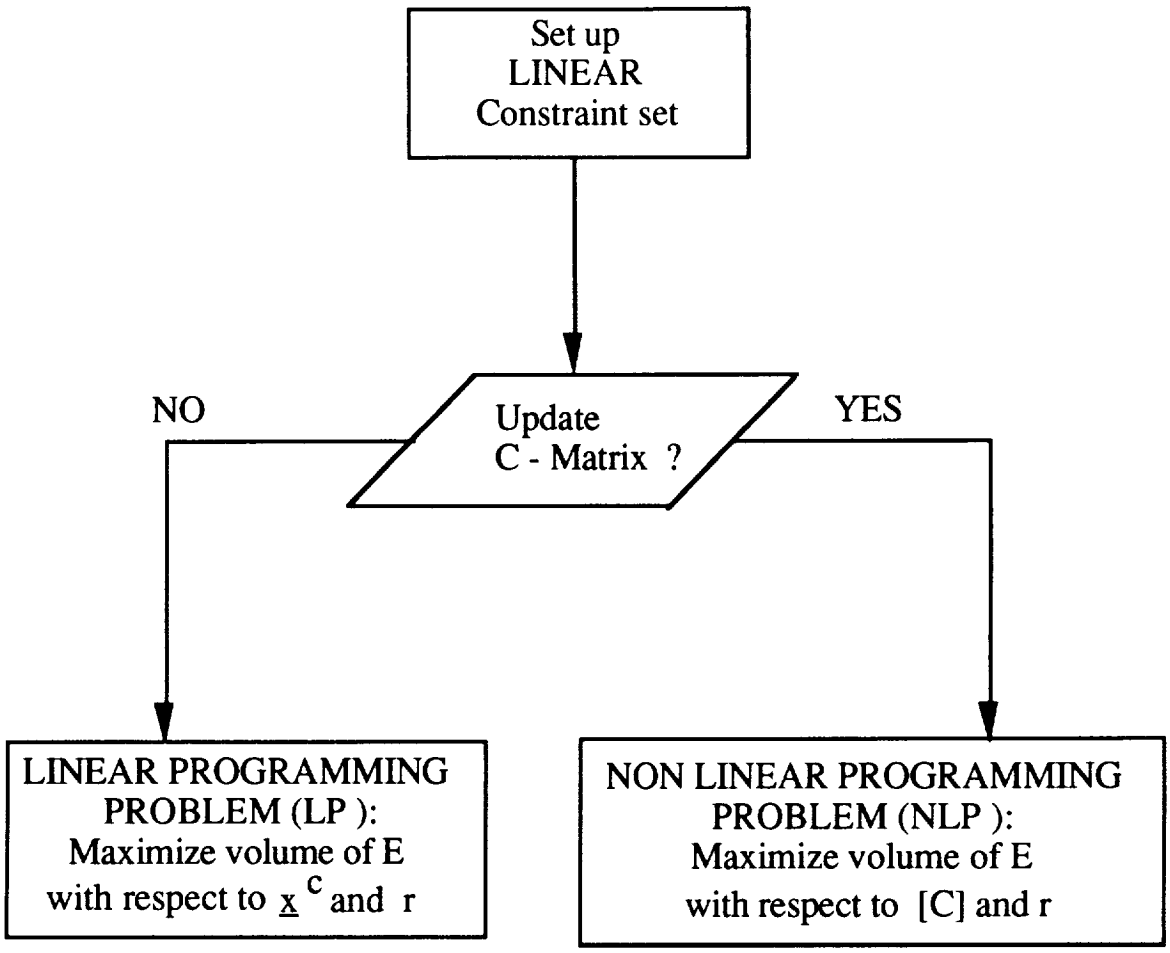

Figure A.2: Method for finding the largest hyperellipse, E, embeded in a polytope R(T)

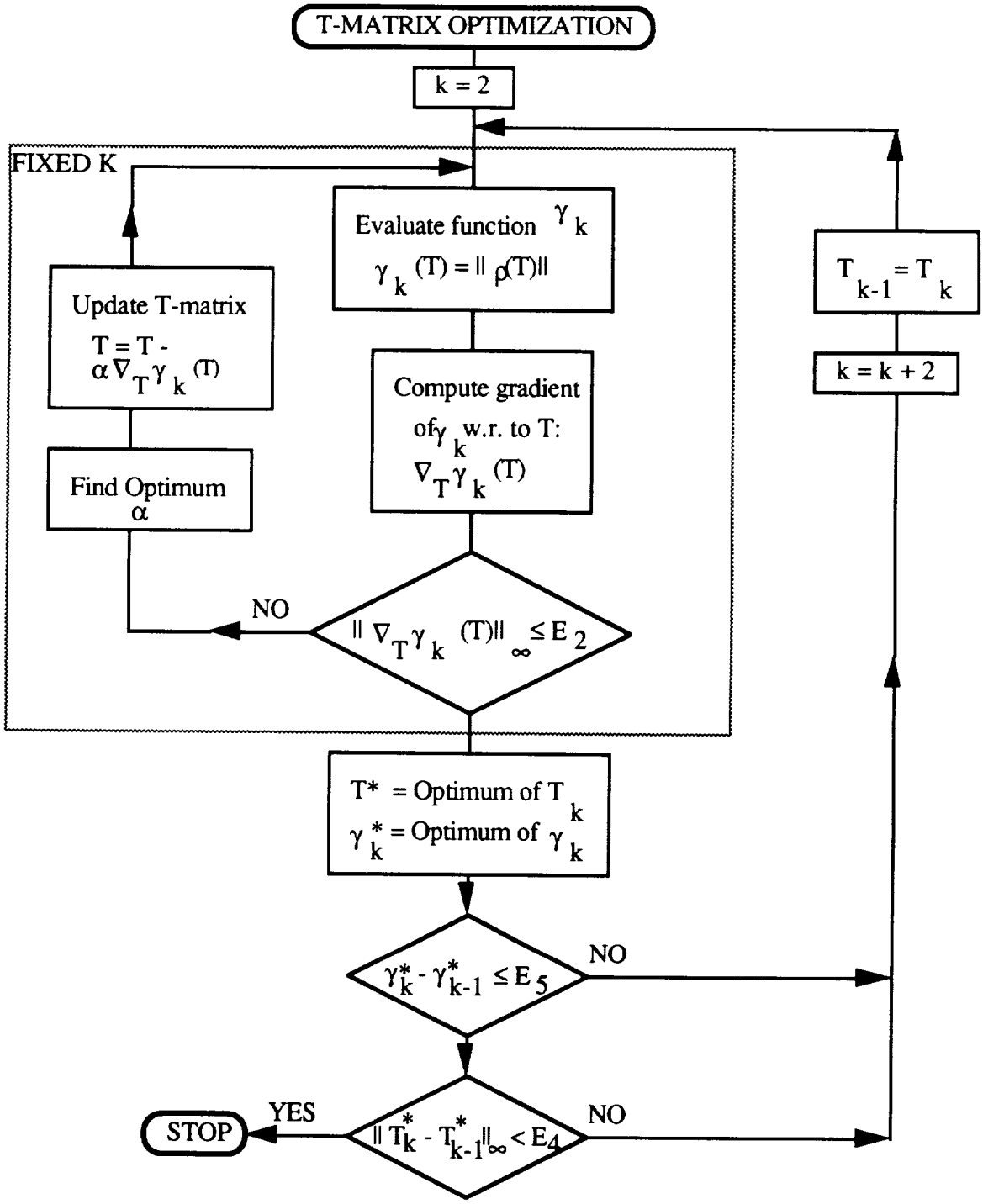

Figure A.3: Flowchart of algorithm for optimizing C-Matrix
(Note - T matrix is the inverse of the C matrix)

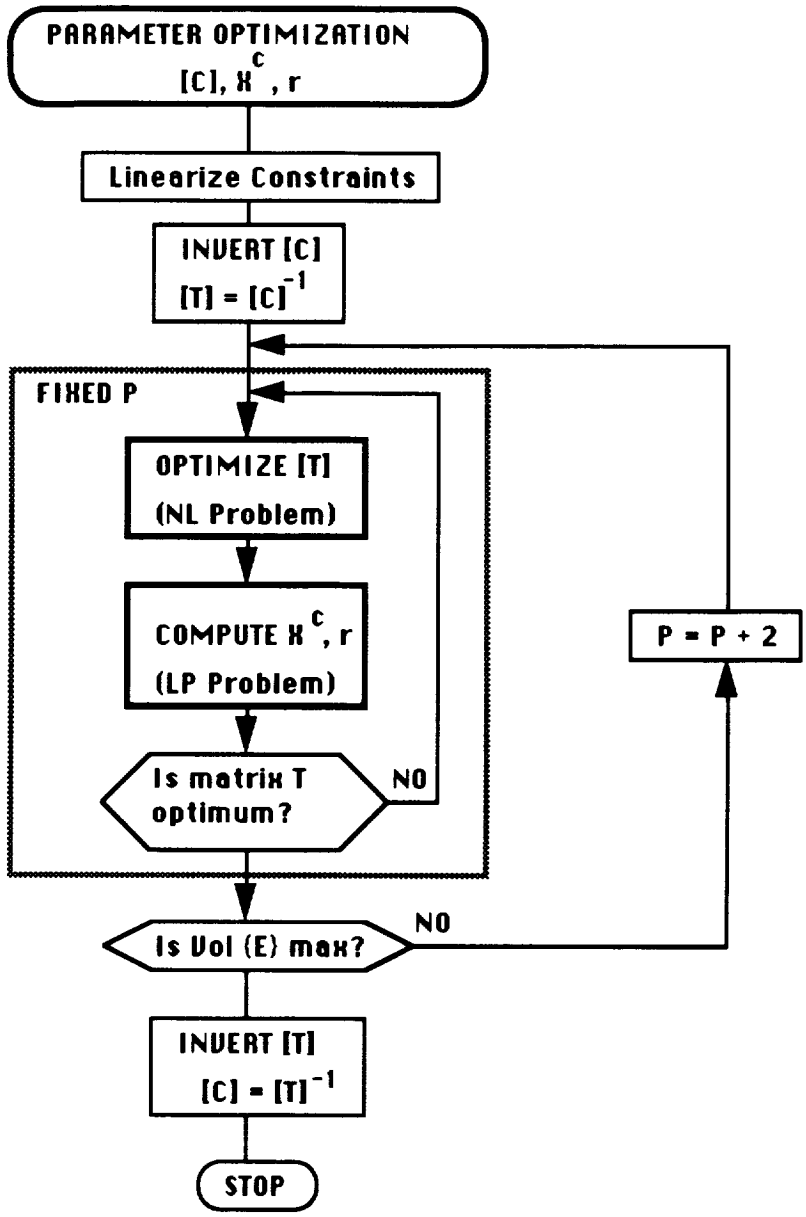

Fig. A.4: Parameter optimization algorithm for computing C-Matrix, center x and radius r